Thermodynamic Model of the System $H^+-NH_4^+-SO_4^{2-}-NO_3^--H_2O$ at Tropospheric Temperatures

Simon L. Clegg* and Peter Brimblecombe

School of Environmental Sciences, University of East Anglia, Norwich NR4 7TJ, U.K.

Anthony S. Wexler

Department of Mechanical Engineering, University of Delaware, Newark, Delaware 19716

Received: September 17, 1997; In Final Form: December 2, 1997

A multicomponent mole-fraction-based thermodynamic model is used to represent aqueous phase activities, equilibrium partial pressures (of H_2O, HNO_3, and NH_3), and saturation with respect to solid phases (H_2SO_4 and HNO_3 hydrates, $(NH_4)_2SO_{4(cr)}$, $(NH_4)_3H(SO_4)_{2(cr)}$, $NH_4HSO_{4(cr)}$, $(NH_4)_2SO_4\cdot 2NH_4NO_{3(cr)}$, $(NH_4)_2SO_4\cdot 3NH_4NO_{3(cr)}$, and $NH_4HSO_4\cdot NH_4NO_{3(cr)}$) in the system $H^+-NH_4^+-SO_4^{2-}-NO_3^--H_2O$. The model is valid from 328 to <200 K, dependent upon liquid-phase composition. Parameters for $H_2SO_4-H_2O$, HNO_3-H_2O, and $(NH_4)_2SO_4-H_2O$ interactions were adopted from previous studies, and values for $NH_4NO_3-H_2O$ obtained from vapor pressures (including data for supersaturated solutions), enthalpies, and heat capacities. Parameters for ternary interactions were determined from extensive literature data for salt solubilities, electromotive forces (emfs), and vapor pressures with an emphasis upon measurements of supersaturated $H_2SO_4-(NH_4)_2SO_4-H_2O$ solutions. Comparisons suggest that the model satisfactorily represents partial pressures of both NH_3 and H_2SO_4 above acidic sulfate mixtures in addition to that of HNO_3, and salt solubilities and water activities.

1. Introduction

Acidic sulfate aerosols occur widely in the troposphere, and an ability to predict their behavior is important for understanding new particle formation,[1,2] urban air quality,[3,4] and atmospheric optical properties.[5]

Such aerosols, particularly those composed mainly of H_2SO_4, are able to remain liquid even at low ambient relative humidities. Furthermore, individual aerosol droplets readily become supersaturated with respect to solid phases in laboratory experiments,[6] and this behavior may also occur in the atmosphere.[7,8] Calculations of the partitioning of water and gases such as HNO_3 and NH_3 into aqueous aerosols and the formation of solids in the aerosol phase require a knowledge of the activities of the aqueous-phase species, Henry's law constants, and other equilibrium constants over the wide range of temperatures experienced in the troposphere. The water content of the aerosols is controlled by the ambient relative humidity, and high aqueous-phase concentrations can be attained at low relative humidities, for the reasons given above. These result in large deviations from ideal solution behavior and make the properties of the system difficult to predict.

Carslaw et al.,[9] using the mole-fraction-based equations of Pitzer, Simonson, and Clegg[10] to calculate activity coefficients, have developed a model of the system $HCl-HNO_3-H_2SO_4-H_2O$ valid from 328 K to less than 200 K. Its primary use is the prediction of gas solubilities in stratospheric aerosols and their composition and physical state.[11] In this work we apply the model to the system $H^+-NH_4^+-SO_4^{2-}-NO_3^--H_2O$. This enables solvent and ion activities, saturation with respect to 13 solid phases, and equilibrium partial pressures of HNO_3 and NH_3 (for acid solutions) to be calculated for temperatures up to 328 K.

2. Theory

In the model, the solvent (water) and all solute (ion) concentrations and activity coefficients are expressed on the mole fraction scale. The mole fraction x_i of species i is given by

$$x_i = n_i/(\sum_j n_j) \tag{1}$$

where n_i is the number of moles of component i and the summation j is over all solution components including the solvent. The activities a_i of all components i are given by $a_i = f_i x_i$, where f_i is the activity coefficient. The reference state for the activity coefficients of solute species is one of infinite dilution with respect to the solvent, denoted by subscript 1. Activity coefficients on this basis (rather than the pure liquid reference state) are denoted f_i^*; thus $f_i^* \rightarrow 1$ as $x_1 \rightarrow 1$. The reference state for the activity coefficient of the pure solvent is the pure liquid, so that $f_1 \rightarrow 1$ as $x_1 \rightarrow 1$. The mole fraction scale activity coefficients given above are, for solute species, related to the more commonly encountered molality-based coefficients γ_i by[12]

$$f_i^* = \gamma_i(1 + (M_1/1000)\sum_i m_i) \tag{2}$$

where M_1 (g mol^{-1}) is the molar mass of the solvent, and m_i (mol per kg of solvent) is the molality of solute species i. The activity coefficient of the solvent, f_1, is related to the rational (mole fraction) osmotic coefficient g and molal osmotic coefficient ϕ by

$$\ln(a_1) = g\ln(x_1) = \ln(x_1) + \ln(f_1) \tag{3a}$$

$$\ln(a_1) = -(M_1/1000)\phi\sum_i m_i \tag{3b}$$

S1089-5639(97)03042-9 CCC: $15.00
Published on Web 02/26/1998

where the summation in eq 3b (as in eq 2) is over all solute species only.

Equilibrium constants, ${}^{x}K$ (on the mole fraction scale), differ from those on the molal scale (${}^{m}K$) for reactions that involve liquid phase solutes by a factor related to the molar mass of the solvent:

$$ {}^{x}K = {}^{m}K(\mathrm{M}_1/1000)^{(\nu_{i,\mathrm{p}}-\nu_{i,\mathrm{r}})} \quad (4) $$

where $\nu_{i,\mathrm{r}}$ is the sum of the stoichiometric numbers of the reacting liquid-phase solutes, and $\nu_{i,\mathrm{p}}$ is the equivalent sum for any products that are also solutes. Thus, for example, for the dissolution of sodium sulfate decahydrate ($Na_2SO_4{\cdot}10H_2O_{(cr)} \rightleftharpoons 2Na^+_{(aq)} + SO_4{}^{2-}_{(aq)} + 10H_2O_{(l)}$) ${}^{x}K$ is equal to ${}^{m}K \times 0.0180152^3$.

The model treats conventional strong electrolytes, such as NaCl and HCl, as fully dissociated in solution. Raman spectral studies have shown that the first dissociation of sulfuric acid ($H_2SO_{4(aq)} = H^+_{(aq)} + HSO_4{}^-_{(aq)}$) is essentially complete at <40 mol kg^{-1} and 298.15 K.[13] However, this is not the case for the second step involving the bisulfate ion, whose dissociation is considered explicitly:[14]

$$ HSO_4{}^-_{(aq)} \rightleftharpoons SO_4{}^{2-}_{(aq)} + H^+_{(aq)} \quad (5) $$

$$ {}^{x}K_{\mathrm{HSO_4}} = a\mathrm{H}^+ a\mathrm{SO_4}^{2-}/a\mathrm{HSO_4}^- \equiv x\mathrm{H}^+ f_{\mathrm{H}}{}^* \, x\mathrm{SO_4}^{2-} f_{\mathrm{SO_4}}{}^*/(x\mathrm{HSO_4}^- f_{\mathrm{HSO_4}}{}^*) \quad (5b) $$

where ${}^{x}K_{\mathrm{HSO_4}}$ is the thermodynamic dissociation constant of $HSO_4{}^-$ on a mole fraction basis, given by eq 6 below:

$$ \log_{10}({}^{x}K_{\mathrm{HSO_4}}) = 560.95050 - 102.5154 \ln(T) - 1.117033 \times 10^{-4} T^2 + 0.2477538T - 13273.75/T \quad (6) $$

where T (K) is temperature. The value of ${}^{x}K_{\mathrm{HSO_4}}$ at 298.15 K is 1.892×10^{-4} (0.0105 mol kg^{-1} on a molality basis).

2.1. Formation of Solid Phases. Consider an aqueous solution containing the cation M and anion X and saturated with respect to salt $M_{\nu+}X_{\nu-}{\cdot}zH_2O_{(cr)}$:

$$ \mathrm{M}_{\nu+}\mathrm{X}_{\nu-}{\cdot}z\mathrm{H_2O}_{(cr)} \rightleftharpoons \nu_+\mathrm{M}_{(aq)} + \nu_-\mathrm{X}_{(aq)} + z\mathrm{H_2O}_{(l)} \quad (7) $$

The equilibrium constant K_S is given by

$$ K_S = a\mathrm{M}^{\nu+} a\mathrm{X}^{\nu-} a_1{}^z / a(\mathrm{M}_{\nu+}\mathrm{X}_{\nu-}{\cdot}z\mathrm{H_2O}_{(cr)}) \quad (8) $$

where aM and aX are the activities of M and X on the appropriate concentration scale, and a_1 is the water activity. The activity of the pure solid phase $a(M_{\nu+}X_{\nu-}{\cdot}zH_2O_{(cr)})$ is by definition unity, leaving only the activity product of the ions and solvent in eq 8. In the systems being treated here there are seven possible solid phases at 298.15 K and several acid hydrates at lower temperatures. Available solubility data have been used to constrain the model, on the basis of the fact that the activity product $a\mathrm{M}^{\nu+}a\mathrm{X}^{\nu-}a_1{}^z$ from eq 8 must have a constant value for any solution saturated with respect to solid $M_{\nu+}X_{\nu-}{\cdot}zH_2O_{(cr)}$ at fixed temperature and pressure, irrespective of solution composition. Values of the equilibrium constants themselves, consistent with the modeled activities, have also been determined in this study.

2.2. Vapor−Liquid Equilibrium. The solubilities of volatile acids such as HNO_3 and HCl in aqueous solution are expressed as the equilibrium

$$ \mathrm{HX}_{(g)} \rightleftharpoons \mathrm{H}^+_{(aq)} + \mathrm{X}^-_{(aq)} \quad (9) $$

with a Henry's law constant ${}^{x}K_{\mathrm{H}}$ (atm^{-1}) on a mole fraction basis defined by

$$ {}^{x}K_{\mathrm{H}} = x\mathrm{H}^+ f_{\mathrm{H}}{}^* \, x\mathrm{X}^- f_{\mathrm{X}}{}^* / p\mathrm{HX} \quad (10) $$

where pHX (atm) is the partial pressure of acid gas HX. (For conversion to SI units, atm = 101 325 Pa.) Note that, strictly, eq 9 combines two equilibria ($HX_{(g)} \rightleftharpoons HX_{(aq)}$, $HX_{(aq)} \rightleftharpoons H^+_{(aq)} + X^-_{(aq)}$). However, descriptions of the thermodynamic properties of strong acids such as HCl and HNO_3 do not require explicit recognition of the undissociated molecule. It is not ignored, but is subsumed into the stoichiometric activity coefficients of the ions in eq 10.

The Henry's law constant of HNO_3 has been evaluated by Clegg and Brimblecombe,[15] using available activity coefficients and partial pressures at 298.15 K, together with enthalpies and heat capacities for the dissolution reaction. An expression for ${}^{x}K_{\mathrm{H}}(HNO_3)$ is given in section 3.2.

It has been suggested that, for aerosols not too acid, equilibrium may be reached between gas-phase NH_3 and dissolved NH_3 within liquid aerosols. Within the context of the model, solutions containing more than one uncharged species (here H_2O and NH_3) should be regarded as being based upon a mixed solvent. However, in atmospheric aerosols the concentration of aqueous ammonia is never likely to be greater than "trace", so the restriction does not in practice apply. Furthermore, dissolved molecular NH_3 will not affect the activities of the other solution components. Thus, it is not necessary to determine NH_3 interactions with other solutes in order to calculate pNH$_3$. We describe the solubility of NH_3 in terms of the equilibrium between the gas phase molecule and aqueous H^+ and $NH_4{}^+$ ions:

$$ \mathrm{NH}_{3(g)} + \mathrm{H}^+_{(aq)} \rightleftharpoons \mathrm{NH_4}^+_{(aq)} \quad (11a) $$

$$ {}^{x}\boldsymbol{K}'_{\mathrm{H}}(\mathrm{NH_3}) = x\mathrm{NH_4}^+ f_{\mathrm{NH_4}}{}^* / (x\mathrm{H}^+ f_{\mathrm{H}}{}^* p\mathrm{NH_3}) \quad (11b) $$

where ${}^{x}\boldsymbol{K}'_{\mathrm{H}}(NH_3)$ (atm^{-1}) is equivalent to the "conventional" Henry's law constant for NH_3 (K'_{H}, for $NH_{3(g)} \rightleftharpoons NH_{3(aq)}$) divided by the acid dissociation constant of $NH_4{}^+$ (K_a, for $NH_4{}^+_{(aq)} \rightleftharpoons H^+_{(aq)} + NH_{3(aq)}$). Here we adopt K_a(298.15 K) equal to 5.6937×10^{-10} mol kg^{-1},[16] K'_{H} (298.15 K) equal to 60.72 mol kg^{-1} atm^{-1},[17] and $\Delta_r H°$ for the reaction in eq 11a equal to −86.25 kJ mol^{-1}.[18,19] A fixed $\Delta_r C_p°$ of 34.35 J mol^{-1} K^{-1} is assumed.[18,20] The equilibrium constant defined by eq 11b is therefore given by

$$ \ln({}^{x}\boldsymbol{K}'_{\mathrm{H}}) = 25.393 + 10373.6(1/T_{\mathrm{r}} - 1/T) + 4.131(T_{\mathrm{r}}/T - (1 + \ln(T_{\mathrm{r}}/T))) \quad (12) $$

where T_r is the reference temperature of 298.15 K.

2.3. The Model. Equations for solute and solvent activity coefficients (and thermal and volumetric properties, if required) are derived from an expression for the excess Gibbs energy of the solution and have been presented for the general case by Clegg et al.[10] This expression consists of an extended Debye−Hückel function (equivalent to that in the molality-based Pitzer model[21]) which accounts for the long-range forces acting in dilute solutions, combined with short-range terms obtained from a Margules expansion in mole fraction.

The model contains interaction parameters whose values must be determined from empirical data. For a single ionic solute

$M_{\nu+}X_{\nu-}$ in water there are parameters B_{MX}, $W_{1,MX}$, $U_{1,MX}$, and $V_{1,MX}$, which account for interactions between the solvent (subscript 1) and ions M and X. As an example, the model equations for water activity (a_1) and the mean mole fraction activity coefficient of the ions ($f^*_{\pm}$) are given below:

$$\ln(a_1) = \ln(x_1) + 2A_x I_x^{3/2}/(1 + \rho I_x^{1/2}) + x_M x_X B_{MX} \exp(-\alpha_{MX} I_x^{1/2}) + x_M x_X B^1_{MX} \exp(-\alpha^1_{MX} I_x^{1/2}) + x_I^2(W_{1,MX} + (x_I - x_1)U_{1,MX}) + 4x_1 x_M x_X(2 - 3x_1)V_{1,MX} \quad (13)$$

$$\ln(f^*_{\pm}) = -z_M z_X A_x[(2/\rho)\ln(1 + \rho I_x^{1/2}) + I_x^{1/2}(1 - 2I_x/(z_M z_X))/(1 + \rho I_x^{1/2})] + 2z_M z_X x_I B_{MX} g(\alpha_{MX} I_x^{1/2})/(z_M + z_X)^2 - x_M x_X B_{MX} \times [z_M z_X g(\alpha_{MX} I_x^{1/2})/(2I_x) + \exp(-\alpha_{MX} I_x^{1/2})(1 - z_M z_X/(2I_x))] + 2z_M z_X x_I B^1_{MX} g(\alpha^1_{MX} I_x^{1/2})/(z_M + z_X)^2 - x_M x_X B^1_{MX} \times [z_M z_X g(\alpha^1_{MX} I_x^{1/2})/(2I_x) + \exp(-\alpha^1_{MX} I_x^{1/2})(1 - z_M z_X/(2I_x))] + x_1(1 - x_I)W_{1,MX} + 2x_1^2 x_I U_{1,MX} + 4x_1^2 x_I(2 - 3x_I)(z_M z_X/(z_M + z_X)^2)V_{1,MX} - W_{1,MX} \quad (14)$$

In the equations, A_x is the Debye−Hückel parameter on a mole fraction basis (2.917 at 298.15 K), I_x is the mole fraction ionic strength, and ρ is a constant. The charge magnitudes of ions M and X are z_M and z_X, respectively. The function $g(x)$ together with terms in B_{MX} and B^1_{MX} and associated coefficients α_{MX} and α^1_{MX} represent the extended Debye−Hückel function. Further terms in x_1 and x_I (the total mole fraction of ions) and parameters $W_{1,MX}$, $U_{1,MX}$, and $V_{1,MX}$ describe the short-range effects that dominate in concentrated solutions. Model expressions for the apparent molar enthalpy ($^{\phi}L$) and heat capacity ($^{\phi}C_p$) of single solute solutions contain the first and second derivatives of the model parameters in eq 13 and eq 14 with respect to temperature.[22]

The values of the parameters for solvent−cation−anion interactions in eq 13 and eq 14 are usually determined from activity coefficient and thermal data for pure aqueous solutions. In multicomponent solutions based on a single solvent and containing several cations (c) and anions (a), in addition to B_{ca}, $W_{1,ca}$, $U_{1,ca}$, and $V_{1,ca}$, parameters of the types $W_{ii'j}$, $Q_{1,ii'j}$, and $U_{ii'j}$ arise where i and i' are dissimilar cations or anions and j is an ion of opposite sign. These have the greatest influence in very concentrated solutions and are typically determined from vapor pressures, electromotive forces (emfs), or salt solubilities for three ion mixtures. The cation−anion coefficients α_{ca} and α^1_{ca} may be either set to fixed values (typically in the range 5−20) or, where necessary, fitted together with the parameters for solvent−cation−anion interactions noted above.

We do not present here equations for activity coefficients, or other thermodynamic properties, of the multicomponent system being studied. This has previously been done in a number of cases for other mixtures,[9,23,24] and readers are referred to Clegg et al.[10] for a full description of the model.

The determination of interaction parameter values is carried out using a nonlinear least-squares fitting routine (E04FDF, from the Numerical Algorithms Group FORTRAN library). Although the terms in eq 13 and eq 14 are defined as describing short- and long-range effects in liquid mixtures, the effects of each extend over the entire concentration range. The parameters are thus quite strongly correlated, and the removal or alteration of the value of one will yield changes, in various degrees, in the others. The determination of parameter values for pure (single solute) aqueous solutions and mixtures is summarized in the following sections.

3. Parameterization of the Model

For the present system both binary and ternary interaction parameters, Henry's law constants of soluble gases, and equilibrium constants for the formation of solid phases are required as a function of temperature. Results for each binary and ternary system are given below. Tables 1 and 2 list the values of model parameters and equilibrium constants determined here.

3.1. $H_2SO_4-H_2O$. Clegg and Brimblecombe[14] have applied the model to this system from 0 to 40 mol kg^{-1} acid, and 328.15 K to <200 K, using measured osmotic coefficients, emfs, degrees of dissociation of the HSO_4^- ion, differential heats of dilution, heat capacities, and freezing points. Coefficients giving the parameters for $H^+-HSO_4^--H_2O$ and $H^+-SO_4^{2-}-H_2O$ interactions as functions of temperature are listed in Table 4 of Clegg and Brimblecombe.[14] Equations for the activity products of sulfuric acid hydrates (^xK_S in eq 8) are given in Table 6 of the same work. The parameterization is the same as that used in the model of Carslaw et al.[9] for stratospheric aerosols and is also adopted here.

3.2. HNO_3-H_2O. Clegg and Brimblecombe[15] have evaluated osmotic and activity coefficients of aqueous HNO_3, and partial molar enthalpies and heat capacities, from 0 to 100 mass % acid at temperatures to 393 K. Carslaw et al.[9] used the results of Clegg and Brimblecombe[15] to parameterize the present model for HNO_3-H_2O solutions from 180 to 330 K and for $x_I < 0.76$ (~88 mol kg^{-1}). Freezing points (with respect to $HNO_3 \cdot 3H_2O_{(cr)}$ and $HNO_3 \cdot H_2O_{(cr)}$) were included in the fit of Carslaw et al.,[9] as were osmotic coefficients at the freezing temperature of the solution (calculated from freezing point depressions, where ice is the precipitating solid phase) in order to constrain the model better at very low temperature. Tables 5 and 6 of Carslaw et al. list coefficients giving the model parameters as functions of temperature and equations for the activity products of solid phases $HNO_3 \cdot H_2O_{(cr)}$ and $HNO_3 \cdot 3H_2O_{(cr)}$. These results are adopted here.

The Henry's law constant of HNO_3 (eq 10) is given by the following expression:[15]

$$\ln[^xK_H(HNO_3)] = 385.972199 - 3020.3522/T - 71.001998\ln(T) + 0.131442311T - 0.420928363 \times 10^{-4}T^2 \quad (15)$$

Equation 15 yields a value of 853.1 atm^{-1} (equivalent to 2.63×10^6 mol^2 kg^{-2} atm^{-1} on a molality basis) at 298.15 K. Predicted partial pressures of HNO_3, using eq 15 for ^xK_H, agree satisfactorily with measured values to the limit of available data at about 215 K.

3.3. $(NH_4)_2SO_4-H_2O$. Clegg et al.[22] have evaluated water and solute activities in aqueous $(NH_4)_2SO_4$ from ~373 K to the eutectic point at 254.21 K, based on isopiestic and electrodynamic balance (edb) measurements, vapor pressures, solubilities, and enthalpies and heat capacities. The data were fitted using parameter values for a reference temperature of 298.15 K, together with enthalpy and heat capacity terms. The inclusion of edb data (obtained for molalities up to about 25 mol kg^{-1}) means that the treatment extends to highly supersaturated solutions for the temperature range over which these measurements were carried out, 278.15−313.15 K.

TABLE 1: Fitted Model Parameters for the System $H^+-NH_4^+-SO_4^{2-}-NO_3^--H_2O$[a]

parameter	value	parameter	value
$B_{NH4\cdot NO3}$	13.0466	$B_{NH4\cdot HSO4}$	$4.95871 + 0.04(T - 298.15)$
$\alpha_{NH4\cdot NO3}$	7.0	$\alpha_{NH4\cdot HSO4}$	13.0
$B^1_{NH4\cdot NO3}$	−16.2254	$W_{NH4\cdot HSO4}$	$-1.63377 - 0.0053933(T - 298.15)$
$\alpha^1_{NH4\cdot NO3}$	13.0	$U_{NH4\cdot HSO4}$	0.362702
$W_{1,NH4\cdot NO3}$	−0.0403564	$V_{NH4\cdot HSO4}$	$0.367167 - 0.0074242(T - 298.15)$
$U_{1,NH4\cdot NO3}$	−0.680507		
$V_{1,NH4\cdot NO3}$	−16.2254	$W_{H\cdot NH4\cdot HSO4}$	$-16.481 + 0.049479(T - 298.15)$
		$Q_{1,H\cdot NH4\cdot HSO4}$	7.0845
$B^L_{NH4\cdot NO3}$	0.283192	$W_{H\cdot NH4\cdot SO4}$	−8.3308
$B^{1,L}_{NH4\cdot NO3}$	−0.0716627	$W_{HSO4\cdot SO4\cdot NH4}$	−8.1710
$W^L_{1,NH4\cdot NO3}$	−0.00696723	$U_{HSO4\cdot SO4\cdot NH4}$	$-11.387 + 0.063352(T - 298.15)$
$U^L_{1,NH4\cdot NO3}$	0.00171736		
$V^L_{1,NH4\cdot NO3}$	0.00221706	$W_{H\cdot NH4\cdot NO3}$	$-4.0728 + 0.042031(T - 298.15) - 3.2245 \times 10^{-4}(T - 298.15)^2$
		$Q_{1,H\cdot NH4\cdot NO3}$	0.75481
$B^J_{NH4\cdot NO3}$	−0.00352077	$U_{H\cdot NH4\cdot NO3}$	−1.0055
$B^{1,J}_{NH4\cdot NO3}$	0.0		
$W^J_{1,NH4\cdot NO3}$	4.89933×10^{-6}	$W_{SO4\cdot NO3\cdot NH4}$	$0.32359 + 0.16567(T - 298.15)$
$U^J_{1,NH4\cdot NO3}$	0.0	$Q_{1,SO4\cdot NO3\cdot NH4}$	$2.6800 - 0.13322(T - 298.15)$
$V^J_{1,NH4\cdot NO3}$	-3.59406×10^{-5}	$U_{SO4\cdot NO3\cdot NH4}$	−0.31582
		$W_{HSO4\cdot NO3\cdot NH4}$	−3.0708

[a] Each parameter P^L and P^J is related to parameter P at the same temperature (here 298.15 K) by $P^L = \partial P/\partial T$, and $P^J = \partial^2 P/\partial T^2 + (2/T)P^L$. Parameters for $H^+-HSO_4^--SO_4^{2-}-H_2O$ (aqueous H_2SO_4) and $NH_4^+-SO_4^{2-}-H_2O$ (aqueous $(NH_4)_2SO_4$) interactions are given by Clegg and Brimblecombe[14] and Clegg et al.,[22] respectively. Ternary parameters for the interactions occurring in $HNO_3-H_2SO_4-H_2O$ mixtures are listed by Carslaw et al.[9] The absolute values of the parameters listed above generally exceed the corresponding errors of estimate (determined in the fitting procedure) by at least a factor of 4, and in most cases by a much larger amount.

TABLE 2: Equilibrium Constants for Solid Phases for the System $H^+-NH_4^+-SO_4^{2-}-NO_3^--H_2O$[a]

solid phase	T_r (K)	$\ln({}^xK_s)$	$\Delta_r H°$ (kJ mol^{-1})	$\Delta_r C_p°$ (J mol^{-1} K^{-1})	$\partial(\Delta_r C_p°)/\partial T$ (J mol^{-1} K^{-2})
$(NH_4)_2SO_4$	298.15	−11.960	6.084	−265.3	−6.393
$(NH_4)_3H(SO_4)_2$	298.15	−26.007	−5.32	−630.4	
NH_4HSO_4	298.15	−11.408	−15.17	−242.3	
NH_4NO_3(V)	256.20	−7.3737	30.41	−101.2	
NH_4NO_3(IV)	298.15	−5.5295	25.69	−101.2	
NH_4NO_3(III)	305.38	−5.2876	23.26	−101.2	
$(NH_4)_2SO_4\cdot 2NH_4NO_3$	298.15	−23.681	58.85		
$(NH_4)_2SO_4\cdot 3NH_4NO_3$	298.15	−29.422	84.86		
$NH_4HSO_4\cdot NH_4NO_3$	298.15	−18.081	8.73		

[a] This table lists thermodynamic quantities for the dissolution of the solid phases, at the reference temperature T_r. In the cases of NH_4NO_3(V) and NH_4NO_3(III) the values of T_r are also the transition temperatures between these crystalline forms and NH_4NO_3(IV).

No extension of the parameterization to stratospheric temperatures, of the kind carried out for HNO_3-H_2O and $HCl-H_2O$ by Carslaw et al.,[9] was attempted. Calculations of the properties of aqueous mixtures containing NH_4^+ and SO_4^{2-} ions for temperatures below about 254 K, for which there are no data for $(NH_4)_2SO_4-H_2O$ solutions, therefore involve the extrapolation of the model.

Parameters determined by Clegg et al.[22] for this system are listed in their Table 3. An expression for ${}^xK_S((NH_4)_2SO_4)$ has also been determined by Clegg et al.,[22] using literature solubilities from 254 to 380 K, and is given below:

$$\ln({}^xK_S((NH_4)_2SO_4)) = -1102.015 + 23931.46/T + 197.3493\ln(T) - 0.384466T \quad (16)$$

We note that new measurements of osmotic coefficients of aqueous $(NH_4)_2SO_4$ solutions at 298.15 and 323.15 K have recently been published.[25] These authors used the molality-based ion-interaction model of Pitzer[21] to represent available data for subsaturated solutions over the same temperature range as studied by Clegg et al.[22] and obtained comparable results.

3.4. $NH_4NO_3-H_2O$. The available thermodynamic data for this system are listed in Table 3. Ammonium nitrate has a high solubility (26.8 mol kg^{-1} at 298.15 K), which increases sharply with temperature to 116.3 mol kg^{-1} at 373.15 K,[26] and aqueous solutions readily supersaturate in droplet form. Chan et al.[27] have used an electrodynamic balance to determine the water activity/composition relationship to over 100 mol kg^{-1} at room temperature.

Values of the model parameters for $NH_4^+-NO_3^--H_2O$ interactions at 298.15 K were first determined by fitting eq 13 to available isopiestic and edb data, yielding an accurate representation of osmotic and activity coefficients to water activities as low as 0.3, with a smooth extrapolation to zero at $x_I = 1$. The result is shown in Figure 1.

Partial molar enthalpies and heat capacities are available up to the saturation molality at 298.15 K, allowing the variation of water and solute activities with temperature to be evaluated over this concentration range. However, as noted above, the solubility of NH_4NO_3 in water rises to about 90% by mass at 373.15 K. This enables measurements of equilibrium water partial pressure and heat capacities at high temperature to be used, by a process of extrapolation, to estimate the solute and solvent activities for solutions that at typical tropospheric temperatures are supersaturated with respect to $NH_4NO_{3(cr)}$. The principal sources of partial pressure data are Campbell et al.,[28]

TABLE 3: Sources of Thermodynamic Data for $NH_4NO_3-H_2O$ Solutions[a]

m[b]			data[d]		
min	max	used[c]	type	t (°C)	source
0.001	0.05	yes	ϕ[e]	25	Hamer and Wu[61]
0.1135	27.072	yes	iso	25	Wishaw and Stokes[62]
0.1081	10.03	no	iso	15, 35	Hejtmankova et al.[37]
4.779	12.641	yes	iso	25	Kirgintsev and Luk'yanov[63]
1.388	112.44	yes	vp	30−90	Campbell et al.[28]
1.388	237.37	yes	vp[f]	0−170	Othmer and Frolich[29]
1.394	29.484	no	vp	51.1−106.8	Sacchetto et al.[30]
sat.	sat.	no[g]	vp	10−40	Apelblat[67]
sat.	sat.	no[g,h]	vp	10−165	Dingemans[72]
25.3	25.3	no	vp	25−60	Emons and Hahn[32]
12.702	111.01	yes	edb[i]	25	Chan et al.[27]
9.196	47.861	yes[j]	sol	−16.8−55	Linke[26]
0.000111	20.0	yes	$^{\phi}L$	25	Parker[31]
0.000111	25.0	yes	$^{\phi}L$	25	Vanderzee et al.[33 k]
0.0	22.2	yes	$^{\phi}C_p$	25	Parker[31]
0.9952	11.956	yes	$^{\phi}C_p$	25	Epikhin et al.[34]
0.03768	22.43	yes	$^{\phi}C_p$[l]	25	Roux et al.[20]
1.388	49.97	yes[m]	C_p	20−80	Gladushko et al.[35]
3.0747	35.688	yes[m]	C_p	sat. −100	Sorina et al.[36]

[a] Boiling point data were not considered. Parameters determined: $B_{NH4\cdot NO3}$, $B^1_{NH4\cdot NO3}$, $W_{1,NH4\cdot NO3}$, $U_{1,NH4\cdot NO3}$, and $V_{1,NH4\cdot NO3}$ including derivatives with respect to temperature (superscripts L and J in Table 1). [b] Molality of NH_4NO_3. [c] Used in the fit of the thermodynamic model. See text for details. [d] Type of data: ϕ, tabulated osmotic coefficient; iso, isopiestic measurements; vp, equilibrium water partial pressures; edb, electrodynamic balance measurements of water activity/concentration relationships for supersaturated solutions; sol, solubility of $NH_4NO_{3(cr)}$, and saturation with respect to ice; $^{\phi}L$, apparent molar enthalpy; $^{\phi}C_p$, apparent molar heat capacity; C_p, heat capacity. [e] These values, from the correlation of Hamer and Wu[61] (which extends to 25.954 mol kg^{-1}), were used to constrain the model at very low molalities. [f] Both the original vapor pressure measurements and values generated from the authors' correlation (80 and 95 wt % NH_4NO_3) were fitted as water activities. Values of L_1 at 25 °C were also calculated from the water partial pressure slopes given by the authors using ΔH°_{vap} for water equal to 44.012 kJ mol^{-1}, but were given a very low weight in the fit of the model. [g] Equilibrium partial pressures of water over solutions saturated with respect to solid NH_4NO_3 and compared with the fitted model (see text). [h] This author also lists the results of five previous studies from the period 1919−1930. [i] Data were restandardized using isopiestic (osmotic coefficient) data from the literature, as described by Clegg et al.[22] for aqueous $(NH_4)_2SO_4$. [j] Used to determine the solubility equilibrium constant ^xK_s. [k] Vanderzee et al.[39] have also determined a standard enthalpy of solution (ΔH°_{soln}) of 25.544 kJ mol^{-1} at 298.15 K. [l] Original data provided by Gerald Perron (personal communication, 1996). [m] Used only to estimate three values of $^{\phi}C_p$ for supersaturated solutions at 298.15 K.

Othmer and Frolich,[29] and Sacchetto et al.[30] (see Table 3). Othmer and Frolich have used their own measurements, those of Campbell et al., and apparent molar enthalpies from Parker[31] to correlate equilibrium water partial pressures for solutions containing from 10 to 95 mass % NH_4NO_3. Values of the partial molar enthalpy of water, L_1, can readily be derived from the expressions of Othmer and Frolich[29] using the relationship $L_1 = (1 - m)\Delta H^\circ_{vap}$, where m is a quantity tabulated by Othmer and Frolich and ΔH°_{vap} is the enthalpy of vaporization of water.

The consistency of the water activities extrapolated from high-temperature data with those from isopiestic and edb measurements at 298.15 K was checked for all the compositions listed by Othmer and Frolich[29] and independently for the data of Campbell et al.;[28] see Figure 2. There is satisfactory agreement for molalities greater than 6.25 mol kg^{-1} (30 mass %), with the exception of values at 12.49 and 112.4 mol kg^{-1} (50 and 90 mass %, respectively). The partial pressure data of Sachetto et al.[30] for 1.394−29.484 mol kg^{-1} NH_4NO_3, when extrapolated to 298.15 K, agreed poorly with other measurements, though

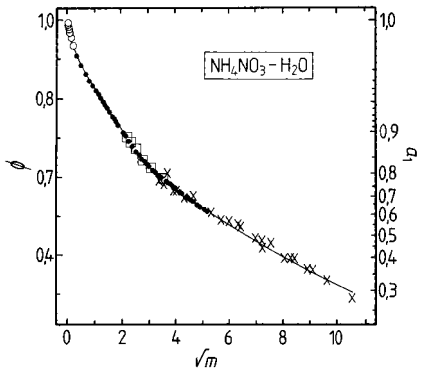

Figure 1. Molal osmotic coefficients (ϕ) of $NH_4NO_{3(aq)}$ at 298.15 K, plotted against the square root of NH_4NO_3 molality (m/mol kg^{-1}). Symbols: open circles, from the evaluation of Hamer and Wu;[61] dots, data of Wishaw and Stokes;[62] open squares, data of Kirgintsev and Luk'yanov;[63] crosses, data of Chan et al.[27] Line: fitted model.

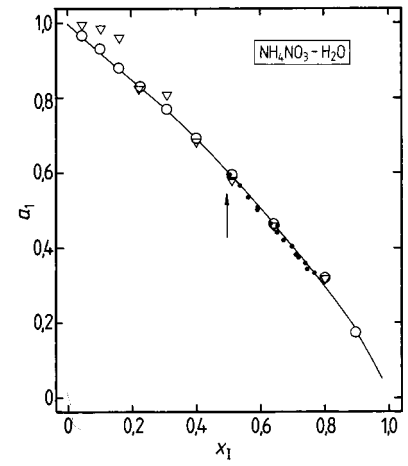

Figure 2. Water activities (a_1) of $NH_4NO_{3(aq)}$ at 298.15 K, plotted against total mole fraction of ions (x_I). The saturated solution composition is marked by a vertical line. Symbols: dots, edb data for supersaturated solutions;[27] open circles, extrapolated using the equations of Othmer and Frolich;[29] open inverted triangles, from the data of Campbell et al.[28] Line: fitted model.

their trend with temperature is generally consistent with the results of Othmer and Frolich[29] (see Figure 6 of Sachetto et al.[30]). The partial pressures determined by Emons and Hahn[32] for 25.3 mol kg^{-1} NH_4NO_3 also exhibit a trend with temperature that agrees well with other data but, when converted to water activities, show a consistent offset of about −0.009, which may be attributable to experimental bias. Neither set of results is further considered here.

Apparent molar enthalpies of aqueous NH_4NO_3 at 298.15 K from the compilation of Parker,[31] representing data up to 1963, agree well with the recent measurements of Vanderzee et al.[33] Apparent molar heat capacities at 298.15 K from the sources listed in Table 3 are consistent with one another, although the measurements of Epikhin et al.[34] are more scattered than those of the other groups. Gladushko et al.[35] and Sorina et al.[36] have measured heat capacities of aqueous NH_4NO_3 over a range of temperatures, and the results were used to estimate values of $^{\phi}C_p$ at 298.15 K up to 49.97 mol kg^{-1}. It is also possible to determine the change of $^{\phi}C_p$ with temperature from these data sets, but this quantity was not needed to represent the measured water partial pressures, and so these additional data were not included in the overall analysis.

Values of the enthalpy parameters and heat capacity parameters for the model (see note to Table 1) were determined by

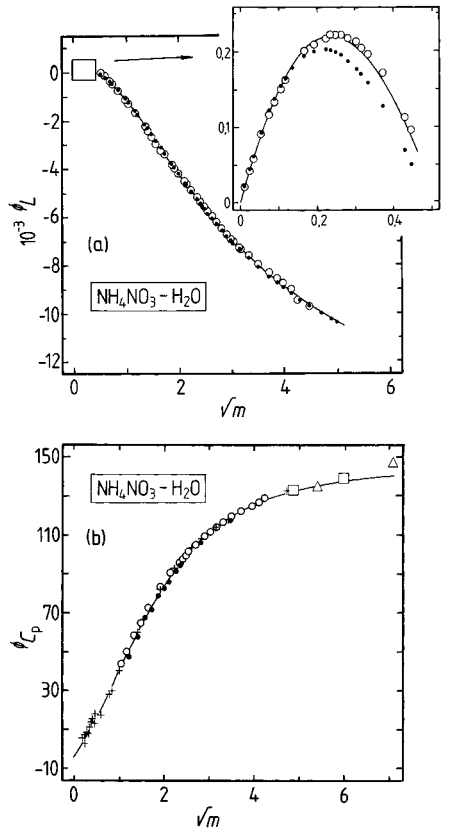

Figure 3. (a) Apparent molar enthalpies ($^{\phi}L$/J mol^{-1}) of $NH_4NO_{3(aq)}$ at 298.15 K, plotted against the square root of NH_4NO_3 molality (m/mol kg^{-1}). Symbols: open circles, from the evaluation of Parker;[31] dots, data of Vanderzee et al.;[33] line, fitted model. The inset shows the data and fit at low concentrations (same scales as the main plot). (b) Apparent molar heat capacities ($^{\phi}C_p$/J mol^{-1} K^{-1}) of $NH_4NO_{3(aq)}$ at 298.15 K, plotted against the square root of NH_4NO_3 molality. Symbols: crosses, data of Roux et al.;[20] open circles, from the evaluation of Parker;[31] dots, data of Epikhin et al.;[34] open squares, estimated from the data of Sorina et al.;[36] open triangles, estimated from the data of Gladushko et al.[35] Line: fitted model.

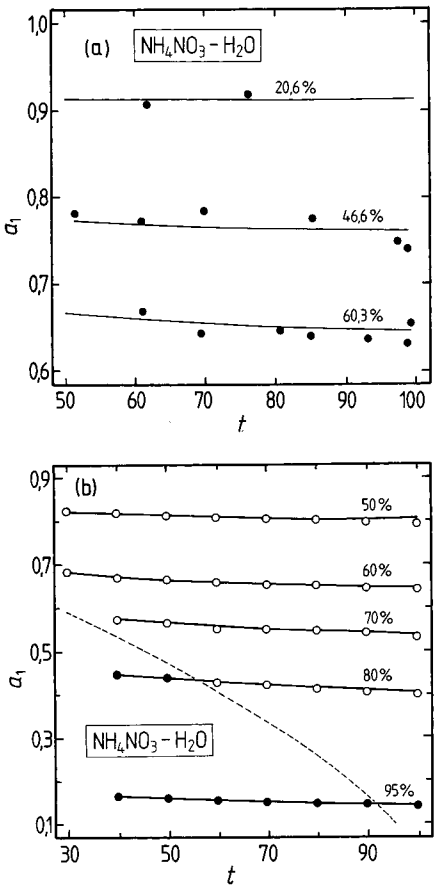

Figure 4. Water activities (a_1) of $NH_4NO_{3(aq)}$ as a function of temperature (t/°C). (a) Symbols: from vapor pressure measurements of Othmer and Frolich[29] for three solution compositions (mass %, indicated on the plot). Lines: fitted model. (b) Symbols: open circles, vapor pressure measurements of Campbell et al.;[28] dots, generated from the fitting equations of Othmer and Frolich.[29] Lines: solid, fitted model; dashed, calculated saturation curve (solutions to the left of this are supersaturated with respect to $NH_4NO_{3(cr)}$ (IV) or (III)).

simultaneously fitting apparent molar enthalpies and heat capacities at 298.15 K, together with water activities derived from the measurements of Campbell et al.[28] for 40−80 mass % NH_4NO_3, and Othmer and Frolich[29] for 20.6−60.3 mass % NH_4NO_3. Further water activities for 80 and 95 mass % solutions, from 313.15 to 373.15 K, were generated using the expressions of Othmer and Frolich and included in the fit. The results are shown in Figures 3 and 4 and demonstrate a satisfactory representation of the available data over a wide temperature range and to high concentration. We also note that the model agrees well with osmotic coefficients at 288.15 and 308.15 K from the isopiestic measurements of Hejtmankova et al.,[37] with deviations of only −0.0038 to +0.004 (288.15 K), and −0.0091 to +0.0049 (308.15 K), for molalities above 1 mol kg^{-1}.

Solubilities of NH_4NO_3 in water are tabulated by Linke,[26] from 256.35 K (eutectic temperature) to 443.15 K, based upon literature data up to 1957. Solid ammonium nitrate occurs in a number of different crystalline forms: orthorhombic (type V) below 256.2 ± 0.4 K, rhombic (type IV) from this temperature to 305.38 ± 0.04 K, and rhombohedral (type III) from 305.38 to 357.25 ± 0.1 K.[38] Two further forms exist at higher temperatures. Nagatani et al.[38] have determined heat capacities of the different solid phases as functions of temperature and the following enthalpies of transition: 473 J mol^{-1} (V to IV) and 1700 J mol^{-1} (IV to III). The solubilities of Linke[26] for solid phases V−III were satisfactorily represented by the model from 256.35 to 333.15 K, using an equilibrium constant of 3.97 × 10^{-3} at 298.15 K and $\Delta_r H°$ (298.15 K) equal to 25.69 kJ mol^{-1} [19] and also including the enthalpies of transition listed above. The enthalpy of solution (25.69 kJ mol^{-1}) agrees well with more recent estimates.[39,40] A single value of $\Delta_r C_p°$ (−101.2 J mol^{-1} K^{-1}) was used for the reaction, as the value of $C_p°$ of the aqueous ions is not known as a function of temperature. We note that this optimized estimate is about 45 J mol^{-1} K^{-1} greater than that derived from the tabulation of Wagman et al.[19] The fit to the data is illustrated in Figure 5, which also compares measured and calculated water partial pressures above saturated solutions of $NH_4NO_{3(aq)}$. Expressions for the equilibrium constants for $NH_4NO_{3(cr)}$ solubility are given in Table 2.

The properties of aqueous NH_4NO_3 are summarized in Figure 6, which shows contours of water activity over a wide range of temperature and to high supersaturation, with the freezing and $NH_4NO_{3(cr)}$ solubility curves superimposed.

3.5. HNO_3−NH_4NO_3−H_2O. The available data sets for this mixture are listed in Table 4 and comprise solubilities (four solid phases), partial pressure, and degree of dissociation measurements. The partial pressure data of Treuschenko et al.[41] are extensive, but also appear to be inaccurate: for example pH_2O values over pure aqueous HNO_3 are too high by 0.001−0.002 atm (2.6%−17%) for 3.89−24.0 mol kg^{-1} acid. Also,

TABLE 4: Sources of Thermodynamic Data for $HNO_3-NH_4NO_3-H_2O$ Solutions[a]

m[b] min	m[b] max	used[c]	data[d] type	t (°C)	source
14.84	>100	yes	sol	0−75	Silcock[53]
0.704	>100	yes	sol	−28.5−100	Kurnakov and Ravitch[43]
0.51	10.82	yes	pK_a*[e]	25	Maeda and Kato[44]
0	85.43	no	pH_2O, $pHNO_3$	30	Treushchenko et al.[41]
18.10	24.00	no	pH_2O, $pHNO_3$	25	Flatt and Benguerel[42]

[a] Parameters determined: $W_{H\cdot NH4\cdot NO3}$, $Q_{1,H\cdot NH4\cdot NO3}$, and $U_{H\cdot NH4\cdot NO3}$. [b] Total molality ($mHNO_3 + mNH_4NO_3$). [c] Used in the fit of the model. [d] Type of measurement: sol, solubility of $NH_4NO_{3(cr)}$, ice, $NH_4NO_3\cdot 2HNO_{3(cr)}$; p$K_a$*, stoichiometric dissociation constant of NH_4^+ in aqueous NH_4NO_3; pH_2O, $pHNO_3$, equilibrium partial pressures. [e] The experimental pK_a* values for NH_4^+ were converted to the quantity $f_{NH_4}^*/f_H^*$ using activity coefficients of NH_3 in $NH_4NO_{3(aq)}$ also determined by Maeda and co-workers.

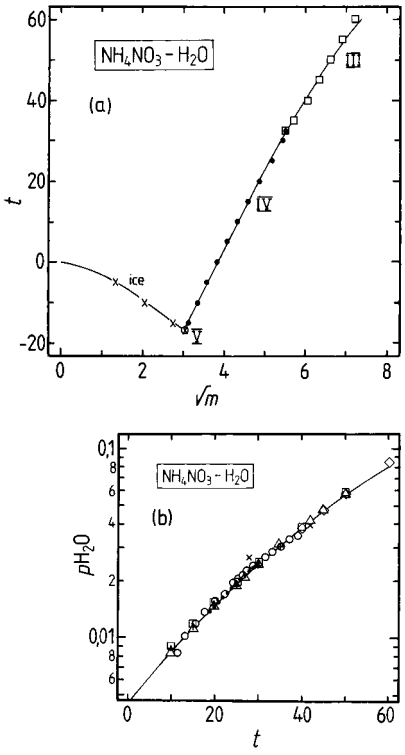

Figure 5. (a) Solubilities of $NH_4NO_{3(cr)}$ (forms III−V) and ice in $NH_4NO_{3(aq)}$ as a function of temperature (t/°C), plotted against the square root of NH_4NO_3 molality (m/mol kg^{-1}). All values are from Linke.[26] Solid phases: crosses, ice; open circle, $NH_4NO_{3(cr)}$ (V); dots, $NH_4NO_{3(cr)}$ (IV); open squares, $NH_4NO_{3(cr)}$ (III); line, fitted model. (b) Equilibrium partial pressures of water (pH_2O/atm) above saturated solutions of NH_4NO_3. Symbols: dots, Edgar and Swan;[64] open diamonds, Prideaux and Caven;[65] pluses, Prideaux;[66] open circles, Apelblat;[67] open squares, Adams and Merz;[68] open triangles, Dingemans;[72] crosses, Janecke and Rahlfs.[69] Line: predicted by the model.

some of the measured $pHNO_3$ values, especially for low HNO_3 molalities, are not consistent with one another. These data were therefore excluded from the fit. The few partial pressure measurements of Flatt and Benguerel[42] were used for comparison only.

The fitted model is based upon the solubility measurements (solid phases ice and $NH_4NO_{3(cr)}$) from 228.15 to 328.15 K and pK_a* of NH_4^+ in aqueous NH_4NO_3 at 298.15 K. Solutions in which $mHNO_3$ was greater than 25 mol kg^{-1} and for which T was greater than 308.15 K were weighted zero in order to optimize agreement with data for lower acidities and temperatures. A high weight was given to the pK_a* measurements (fitted as $f_{NH_4}^*/f_H^*$), as these are relevant to the most common atmospheric case of an aerosol containing significant quantities of NH_4^+ and NO_3^-, but only a small amount of hydrogen ion. The results of the model fit are shown in Figures 7−9. The

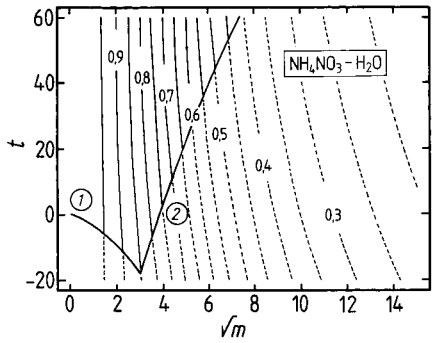

Figure 6. Phase diagram of NH_4NO_3 solutions as a function of temperature (t/°C) and equilibrium water activities for both subsaturated and supersaturated solutions. Compositions are plotted as the square root of molality (m/mol kg^{-1}). Lines: solid (heavy), solubilities of the following solid phases: (1) ice; (2) $NH_4NO_{3(cr)}$. Contours: equilibrium water activities, with values as marked. Contours are dotted for supersaturated solutions.

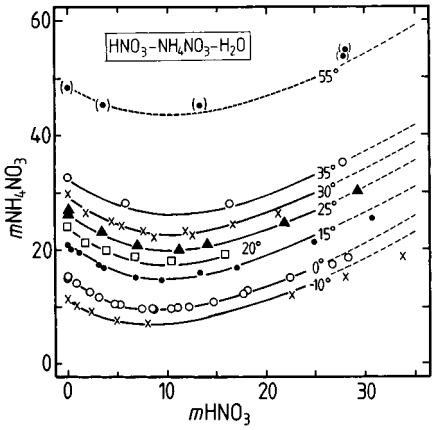

Figure 7. Solubility of $NH_4NO_{3(cr)}$ in $HNO_{3(aq)}$ at different temperatures (°C, as marked on the plot). Data are plotted as molalities (mol kg^{-1}). Symbols: data from Silcock[53] and Kurnakov and Ravitch.[43] Lines: the fitted model. The fit was restricted to a maximum HNO_3 molality of 25 mol kg^{-1} and to a maximum temperature of 308.15 K. The dotted lines show model extrapolations for higher concentrations and temperatures.

solubilities of $NH_4NO_{3(cr)}$ in $HNO_{3(aq)}$ (Figure 7) show strong "salting-in" above about 10 mol kg^{-1} HNO_3. Model calculations show that in this composition region the addition of NH_4NO_3 to the aqueous solution decreases the HNO_3 partial pressure despite the higher concentration of NO_3^- ion. This result is consistent with the partial pressure measurements of Treushchenko et al.[41] and those of Flatt and Benguerel[42] (see Figure 10).

Solubilities below 273.15 K, Figures 7 and 8, are represented well. This result, and earlier work for HNO_3-H_2O solutions,[9] suggests that the model predicts the phase diagram at low

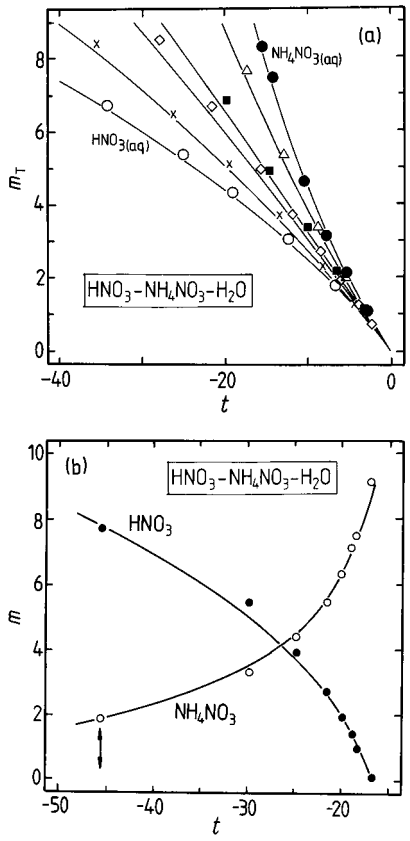

Figure 8. (a) Saturation of $HNO_3-NH_4NO_3-H_2O$ mixtures with respect to ice as a function of temperature (t/°C) and total molality (m_T, equal to $mHNO_3 + mNH_4NO_3$). Results are shown for six composition ratios, r (equal to mNH_4NO_3/m_T). Data are from Kurnakov and Ravitch.[43] Symbols: dots, $r = 1.0$; open triangles, $r = 0.796$; solid squares, $r = 0.529$; open diamonds, $r = 0.423$; crosses, $r = 0.223$; open circles, $r = 0.0$; lines, fitted model. (b) Simultaneous saturation of $HNO_3-NH_4NO_3-H_2O$ mixtures with respect to ice and $NH_4NO_{3(cr)}$ as a function of temperature (t/°C) and molalities (m) of HNO_3 and NH_4NO_3. Data are from Kurnakov and Ravitch.[43] Symbols: dots, HNO_3 molality in the mixtures; open circles, NH_4NO_3 molality in the mixtures. Lines: fitted compositions. The vertical arrow marks the temperature and composition at which the solution becomes saturated with respect to $HNO_3 \cdot 3H_2O_{(cr)}$. This point is satisfactorily predicted by the model.

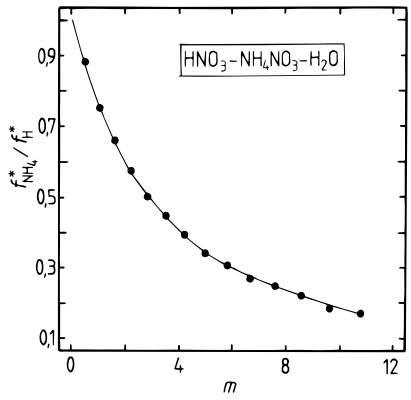

Figure 9. Reciprocal of NH_4^+ and H^+ activity coefficients in $NH_4NO_{3(aq)}$, determined from pK_a* measurements at 298.15 K, and plotted against NH_4NO_3 molality (m/mol kg^{-1}). Symbols: data of Maeda and Kato.[44] Line: fitted model.

temperatures satisfactorily within the limits of the parameterization (88 mol kg^{-1} for HNO_3-H_2O, but probably a much lower molality for NH_4NO_3 at $T \ll 298.15$ K). We note that, at 263.15 K and for concentrations of about 68 mol kg^{-1} HNO_3 and 25−40 mol kg^{-1} NH_4NO_3, the solid-phase $NH_4NO_3 \cdot 2HNO_{3(cr)}$ is formed.[43] This phase has not been included in the model, because it is unlikely to occur in atmospheric aerosols due to the very high concentrations of aqueous-phase HNO_3 required.

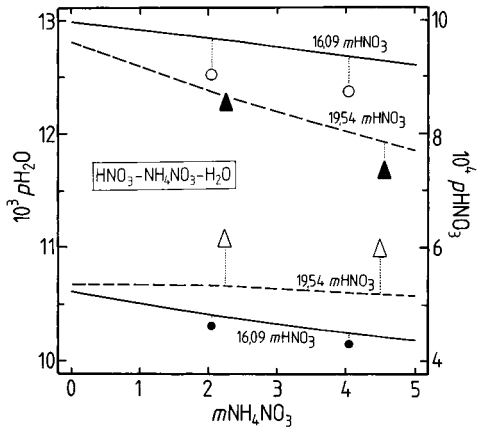

Figure 10. Equilibrium partial pressures of H_2O and HNO_3 (atm) above $HNO_3-NH_4NO_3-H_2O$ solutions, as a function of NH_4NO_3 molality, for two different HNO_3 molalities (indicated on the plot). The data are from Flatt and Benguerel.[42] Symbols: open circles and open triangles, pH_2O; dots and solid triangles, $pHNO_3$. Lines: solid, fitted model (for solutions containing 16.09 mol kg^{-1} HNO_3); dashed, fitted model (for solutions containing 19.54 mol kg^{-1} HNO_3); fine dotted, these associate the data points with the corresponding fitted lines.

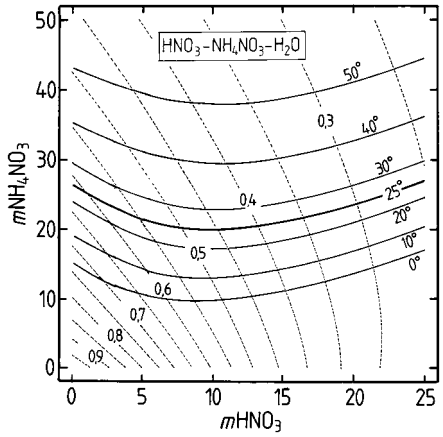

Figure 11. Calculated solubilities of $NH_4NO_{3(cr)}$ in $HNO_{3(aq)}$ from 273.15 to 323.15 K, and equilibrium water activities for both subsaturated and supersaturated solutions at 298.15 K. Compositions are given as molalities. Lines: solid (heavy), solubilities of $NH_4NO_{3(cr)}$, Celsius temperatures as marked; dashed (fine), contours of water activity (a_1) at 298.15 K, values as marked.

The measurements of Maeda and Kato,[44] Figure 9, show that the activity coefficients of NH_4^+ and H^+ differ by about a factor 5 in 10 mol kg^{-1} NH_4NO_3 at 298.15 K. The change in $f_{NH_4}*/f_H*$ with salt concentration is accurately represented by the model. Calculated water activities and solubilities of $NH_4NO_{3(cr)}$ are shown in Figure 11.

3.6. $HNO_3-H_2SO_4-H_2O$. Carslaw et al.[9] have evaluated model parameters for this acid mixture, based principally upon HNO_3 partial pressures measured by Vandoni[45] at 273.15 K and at lower temperatures by Zhang et al.[46] and freezing points with respect to various H_2SO_4 and HNO_3 hydrates. Sources of data are listed in Table 11 of Carslaw et al.[9] The parameterization of these authors is adopted here, and values of $W_{HSO4,NO3,H}$, $W_{SO4,NO3,H}$, and $U_{HSO4,NO3,H}$ are listed in Table 1.

3.7. $H_2SO_4-(NH_4)_2SO_4-H_2O$. This system has previously been modeled by Clegg and Brimblecombe,[23] at 298.15 K only,

TABLE 5: Sources of Thermodynamic Data for Aqueous $(NH_4)_2SO_4-H_2SO_4-H_2O$ Mixtures[a]

m^b min	m^b max	composition	used[c]	data type[d]	t (°C)	source
1.54	8.76	letovicite[e]	yes	vp	20−30	Tang et al.[70]
5.71	28.92	letovicite	no	edb	25	Tang and Munkelwitz[6]
1.75	8.56[f]	letovicite	no	vp	25	Tang and Munkelwitz[6]
6.08	70.9	$(NH_4)_{1.42}H_{0.58}SO_4$	yes	edb	*g*	Spann[48]
h		variable	yes	sol	0−50	Silcock[53]
0.23	6.85	variable	no[i]	iso	15	Park et al.[50]
2.74	110.6[j]	variable	no[i]	edb	*g*	Spann[48]
5.663	30.98[k]	variable	no[i]	edb	*g*	Spann[48]
0.145	7.472[l]	*m*	yes	iso	25,50	Clegg et al.[25]
1.132	24.98[n]	NH_4HSO_4	yes	vp	25	Tang and Munkelwitz[51]
5.578	>100	NH_4HSO_4	no	edb	25	Tang and Munkelwitz[6]
14.06	90.78[o]	NH_4HSO_4	yes	edb	25	Spann[48]
4.97	>100	NH_4HSO_4	no[p]	edb	25	Kim et al.[49]
0.21	10.1	NH_4HSO_4	yes	α	0−50	Young et al.[13]
0.23	10.4	NH_4HSO_4	no	α	25	Irish and Chen[73]
0.66	8.61	NH_4HSO_4	yes	α	25,50	Dawson et al.[71]
0.5	2.5	NH_4HSO_4	no	α	25,55	Kruus et al.[74]
5.61	>100	*q*	no[p]	edb	25	Kim et al.[49]

[a] Balej et al.[75] have measured degrees of dissociation of HSO_4^- for mixtures of various compositions at 293.15 K, but these are not considered here. Imre et al.[76] have recently measured water activities of aqueous NH_4HSO_4 particles and solid−liquid phase transitions to low temperature. These results are briefly discussed in section 3.7. Parameters determined: $B_{NH4\cdot HSO4}$, $W_{1,NH4\cdot HSO4}$, $U_{1,NH4\cdot HSO4}$, $V_{1,NH4\cdot HSO4}$, $W_{H\cdot NH4\cdot HSO4}$, $Q_{1,H\cdot NH4\cdot HSO4}$, $W_{H\cdot NH4\cdot SO4}$, $W_{HSO4\cdot SO4\cdot NH4}$ and $U_{HSO4\cdot SO4\cdot NH4}$. [b] Total molality ($m H_2SO_4 + m(NH_4)_2SO_4$). [c] Used in the fit of the model. [d] Type of measurement: vp, water partial pressure; edb, electrodynamic balance measurements of water activity/concentration relationships for supersaturated solutions; sol, solubility of $(NH_4)_2SO_{4(cr)}$, $(NH_4)_3H(SO_4)_{2(cr)}$ (letovicite), and $NH_4HSO_{4(cr)}$; iso, isopiestic measurement; α, degree of dissociation of HSO_4^-. [e] Values used here were extracted from the graphs presented by Tang et al.[70] [f] Incorrectly identified as being from Tang et al.[70] [g] The measurements were carried out at room temperature, which we have treated here as being 298.15 K. The single rejected point for the second data set contained >50 mol kg^{-1} $(NH_4)_2SO_4$. The thesis of Spann also contains other data for the $(NH_4)_2SO_4-H_2SO_4-H_2O$ system, for example water activities of various saturated aqueous mixtures. [h] Compositions up to 100% $H_2SO_4 + (NH_4)_2SO_4$ and saturation with respect to solid phases $(NH_4)_2SO_{4(cr)}$, $(NH_4)_3H(SO_4)_{2(cr)}$ (letovicite), $NH_4HSO_{4(cr)}$, and $NH_4H_3(SO_4)_{2(cr)}$. The number of data points refers to those for which $t \leq 50$ °C. [i] These data were used for testing the model and not for parameterization. Number of observations for data set 4 refers only to mixtures and not to pure aqueous H_2SO_4 or $(NH_4)_2SO_4$. [j] Total molality, $m(NH_4)_2SO_4 + m NH_4HSO_4$. These data are drawn from Figure 14 of Spann's thesis. [k] Total molality, $m(NH_4)_2SO_4 + m NH_4HSO_4$. These data are taken from Table 3 of Spann's thesis. [l] Thirty five values of ϕ for aqueous NH_4HSO_4 at 298.15 K (calculated using the model of Clegg et al., 1996) and a further 69 estimates of ϕ at 323.15 K (generated by interpolation of the measurements of Clegg et al.[25]) were also included in the fit. [m] Measurements for ratios 2:1 and 1:2 $(NH_4)_2SO_4/H_2SO_4$. [n] Figure 4 in Tang and Munkelwitz[51] also shows the temperature variation of the water vapor pressure at four fixed wt % concentrations of NH_4HSO_4. [o] These data are drawn from Figure 16 of Spann's thesis.[48] The measurements were carried out at room temperature, which we have treated here as being 298.15 K. [p] These edb data were not fitted, but were found to agree well with the model, and with other measurements, for $(NH_4)_2SO_4/H_2SO_4$ ratios 1:2 and 1:1 (NH_4HSO_4). However, the results of Kim et al. for mixtures containing mostly $(NH_4)_2SO_4$ are discordant with other edb measurements. [q] Composition ratios 2:1 and 1:2 $(NH_4)_2SO_4/H_2SO_4$.

using the $H_2SO_4-H_2O$ parameterization of Clegg and Brimblecombe[14] and values for $(NH_4)_2SO_4-H_2O$ determined from a fit to the available isopiestic data and edb measurements of Richardson and Spann.[47] The parameter set for the mixed solutions was based chiefly on solubility and isopiestic data for subsaturated solutions and the edb results of Spann.[48] The sources of data used by Clegg and Brimblecombe[23] are listed in their Tables 1−3. Recently, Clegg et al.[22] have evaluated the thermodynamic properties of aqueous $(NH_4)_2SO_4$ to high supersaturation as a function of temperature, and further edb and isopiestic studies of the acid sulfate mixture have been carried out at 298.15 and 323.15 K.[25,49] The sources of currently available thermodynamic data are listed in Table 5.

Isopiestic and edb measurements for $H_2SO_4-(NH_4)_2SO_4-H_2O$ are restricted to 298.15 and 323.15 K, with measurements of the degree of dissociation of HSO_4^- also available at these temperatures and at 273.15 K. Solubilities of solid phases $(NH_4)_2SO_{4(cr)}$, $(NH_4)_3H(SO_4)_{2(cr)}$ (letovicite), $NH_4HSO_{4(cr)}$, and $NH_4H_3(SO_4)_{2(cr)}$ have been determined over a wider range of temperatures ($T \geq 273.15$ K). The unknown model parameters for this system include those for $NH_4^+-HSO_4^-$ interactions and a number of "mixture" parameters that involve three ions. These were determined by fitting the data and at the same time determining equilibrium constants for the formation of letovicite and ammonium bisulfate as a function of temperature. Saturation with respect to the solid-phase $NH_4H_3(SO_4)_{2(cr)}$ was not treated, as this precipitates only from solutions containing very high concentrations of H_2SO_4 (greater than about 80 mol kg^{-1} H_2SO_4, beyond the upper limit of validity of the model), for which water activities are extremely low. As noted in Table 5, some calculated osmotic coefficients from the model of Clegg et al.[25] and interpolated values (also based on the results of that study) were included in the fit to constrain better the model.

Vapor pressure data for different solution compositions are compared in Figures 12−14. Osmotic coefficients for solutions of letovicite composition are shown in Figure 12 and include values interpolated from the studies of Park et al.[50] and Spann.[48] The results of the fitted model and that of Clegg et al.[25] are also shown. With the exception of the vapor pressures of Tang and Munkelwitz[6] (appearing as crosses in Figure 12), there is good overall agreement. Data for mixtures containing two lower ratios of NH_4^+ to H^+ (2.448:1 and 1.945:1), compared in Figure 13, are also consistent with one another and agree well with the fitted model. However, we note that the results of Kim et al.[49] for 2:1 NH_4^+/H^+ (not shown) are highly discordant with other data, with water activities that are too low by about 0.05 at 10 mol kg^{-1} and by more than 0.1 at 30 mol kg^{-1} total molality.

Measurements for aqueous NH_4HSO_4 are shown in Figure 14. The vapor pressure data of Tang and Munkelwitz[51] and interpolated isopiestic measurements of Park et al.[50] agree well. However, osmotic coefficients from the edb data of Kim et al.[49] and Tang and Munkelwitz[6] differ by up to 0.15 at ∼10 mol kg^{-1} ($\Delta a_1 \simeq 0.05$). Electrodynamic balance measurements from

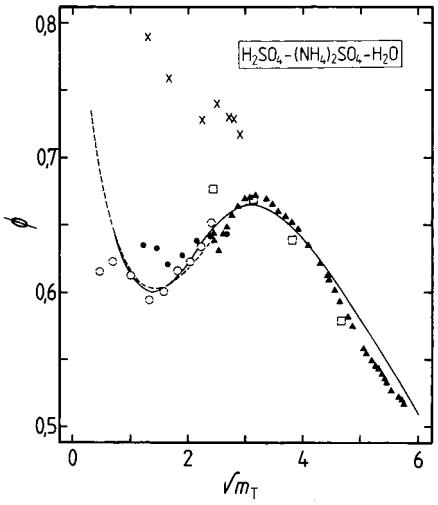

Figure 12. Comparison of stoichiometric molal osmotic coefficients (ϕ) of $(NH_4)_3H(SO_4)_{2(aq)}$ at 298.15 K, plotted against the square root of total molality (m_T, equal to $mH_2SO_4 + m(NH_4)_2SO_4$). Symbols: dots, vapor pressure data of Tang et al.;[70] broken circles, interpolated from the isopiestic measurements of Park et al.;[50] broken squares, interpolated from the edb data of Spann;[48] crosses, vapor pressure measurements of Tang and Munkelwitz;[6] solid triangles, edb data of Tang and Munkelwitz[6] (restandardised in this work). Lines: solid, fitted model; dashed, model of Clegg et al.[25]

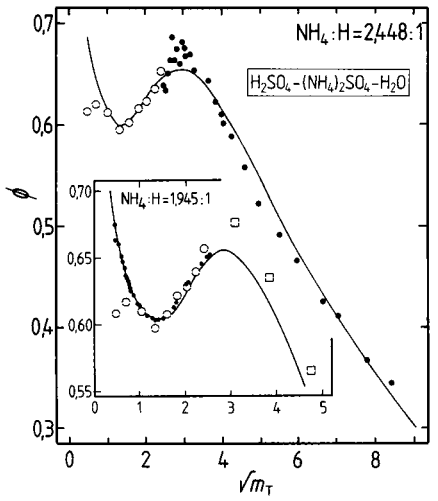

Figure 13. Comparison of stoichiometric molal osmotic coefficients (ϕ) of $H_2SO_4-(NH_4)_2SO_4-H_2O$ at 298.15 K, for two compositions, plotted against the square root of total molality (m_T, equal to $mH_2SO_4 + m(NH_4)_2SO_4$). Main plot ($NH_4^+/H^+ = 2.448:1$): dots, edb data of Spann;[48] broken circles, interpolated from the isopiestic measurements of Park et al.;[50] line, fitted model. Inset ($NH_4^+/H^+ = 1.945:1$): dots, isopiestic data of Clegg et al.;[25] broken circles, interpolated from the isopiestic measurements of Park et al.;[50] broken squares, interpolated from the edb data of Spann;[48] line, fitted model.

all three sources agree at higher molalities up to about $m_T = 35$ mol kg^{-1}, but beyond this the results of Tang and Munkelwitz[6] yield consistently higher osmotic coefficients. This is qualitatively similar to differences noted for aqueous $(NH_4)_2SO_4$ (Figure 15 of Clegg et al.[22]). For NH_4HSO_4 solutions, the fit of the model was based upon the edb measurements only of Spann[48] and agrees closely with those data; see Figure 14.

The results of the fits to other measurements are shown in Figures 15−20, with model parameters and expressions for the equilibrium constants of the solid phases given in Tables 1 and 2. We note that the results for the dissociation constant of the HSO_4^- ion in aqueous NH_4HSO_4 (Figure 19) show that the model predicts values that are too low at high concentrations

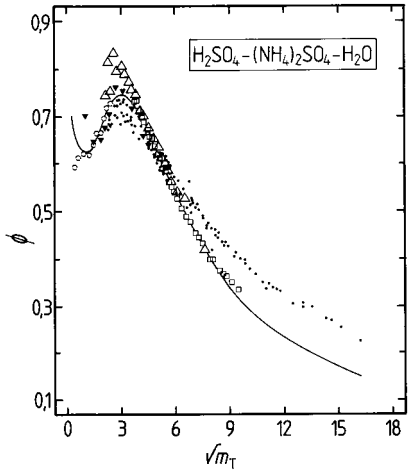

Figure 14. Comparison of stoichiometric molal osmotic coefficients (ϕ) of $NH_4HSO_{4(aq)}$ at 298.15 K, for two compositions, plotted against the square root of total molality (m_T, here equal to mNH_4HSO_4). Symbols: dots, edb data of Tang and Munkelwitz;[6] broken circles, interpolated from the isopiestic measurements of Park et al.;[50] open triangles, edb data of Kim et al.;[49] open squares, edb data of Spann;[48] inverted solid triangles, vapor pressure measurements of Tang and Munkelwitz.[51] Line: fitted model.

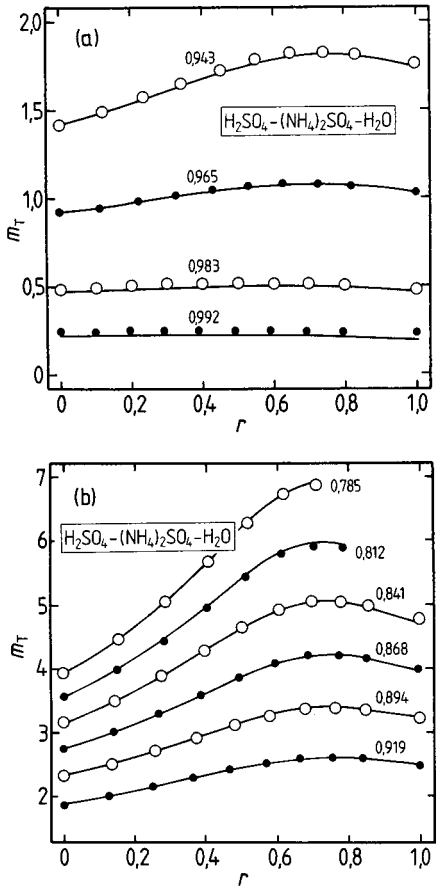

Figure 15. Total molalities (m_T) of $(NH_4)_2SO_4-H_2SO_4-H_2O$ mixtures at 298.15 K, plotted against the solute fraction of $(NH_4)_2SO_4$ [r, equal to $m(NH_4)_2SO_4/(mH_2SO_4 + m(NH_4)_2SO_4)$]. Values of m_T are plotted for constant water activities (a_1) which are indicated on the figure. Symbols: isopiestic data of Park et al.[50] Lines: fitted model. (a) $0.0 \le m_T \le 2.0$ mol kg^{-1}; (b) $2.0 \le m_T \le 7.0$ mol kg^{-1}.

at 298.15 K. This is similar to the result obtained by Clegg and Brimblecombe.[23] However, such errors in the speciation are not reflected in values of the ionic activities or the water

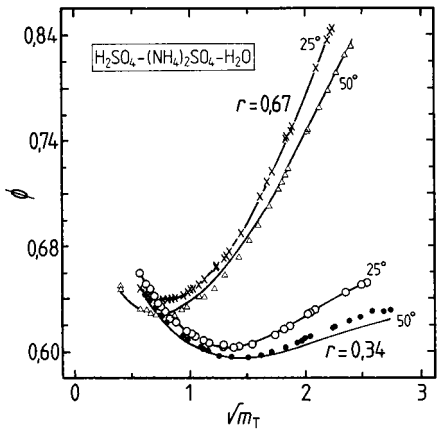

Figure 16. Stoichiometric molal osmotic coefficients (ϕ) of $H_2SO_4-(NH_4)_2SO_4-H_2O$ mixtures at 298.15 and 323.15 K, plotted against the square root of total molality (m_T, equal to $mH_2SO_4 + m(NH_4)_2SO_4$). Symbols: data of Clegg et al.[25] for two composition ratios r (equal to $mH_2SO_4/(mH_2SO_4 + m(NH_4)_2SO_4)$), and two Celsius temperatures (marked). Lines: fitted model.

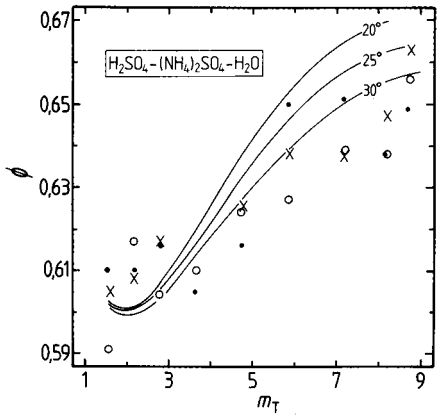

Figure 17. Stoichiometric molal osmotic coefficients (ϕ) of $(NH_4)_3H(SO_4)_{2(aq)}$ from 293.15 to 303.15 K, plotted against the square root of total molality (m_T, equal to $mH_2SO_4 + m(NH_4)_2SO_4$). Data are those of Tang et al.[70] Symbols: dots, 293.15 K; open circles, 298.15 K; crosses, 303.15 K. Lines: fitted model.

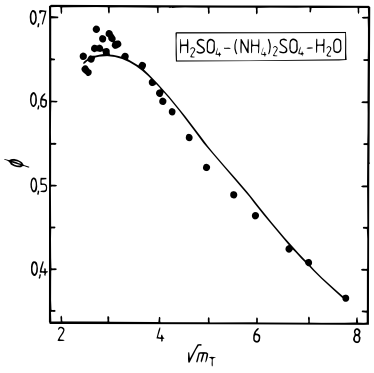

Figure 18. Stoichiometric molal osmotic coefficients (ϕ) of $(NH_4)_{1.42}H_{0.58}SO_{4(aq)}$ at 298.15 K, plotted against the square root of total molality (m_T, equal to $mH_2SO_4 + m(NH_4)_2SO_4$). Symbols: data of Spann.[48] Line: fitted model.

activity (Figures 14 and 15) and so are likely to have little practical effect.

The recent experimental study of phase equilibria of aqueous NH_4HSO_4 particles to low temperature by Imre et al.[76] includes an equilibrium phase diagram (their Figure 4). This shows a transition from aqueous solution to solid NH_4HSO_4 for concentrations greater than about 40 wt % NH_4HSO_4. However,

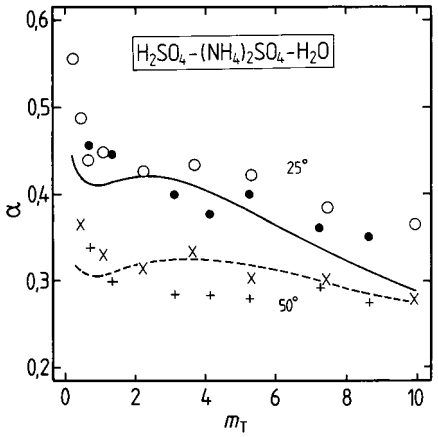

Figure 19. Degrees of dissociation of HSO_4^- ion (α) in $NH_4HSO_{4(aq)}$ at 298.15 and 323.15 K, plotted against total molality (m_T, equivalent to mNH_4HSO_4). Symbols: open circles, data of Young et al.[13] (298.15 K); dots, data of Dawson et al.[71] (298.15 K); crosses, data of Young et al.[13] (323.15 K); pluses, data of Dawson et al.[71] (323.15 K). Lines: fitted model.

it is apparent from the bulk solution data shown in Figure 20 that the transition should occur in two stages: first the precipitation of letovicite as an NH_4HSO_4 solution becomes more concentrated in response to a decrease in relative humidity (hence water activity). Second, the composition of the remaining liquid phase should follow curve 2 in Figure 20 until a final transition to a dry particle at a relative humidity corresponding to that at the apex where saturation curves 2 and 3 meet. The phase transition plotted by Imre et al. corresponds closely to that calculated by the model for the onset of letovicite precipitation. Given that the two stage transitions described above may not be observed in single-particle experiments (where metastable states often occur), this suggests satisfactory agreement between the model and measurements. Figure 4 of Imre et al.[76] also shows phase transitions for ice and $NH_4HSO_4 \cdot 8H_2O$ (a previously unknown hydrate). Results for the former are highly discordant with the temperature trend in water activities obtained from isopiestic data at 298.15 and 323.15 K. The model predicts much smaller freezing point depressions than obtained by Imre et al.,[76] with an ice/letovicite coexistence point corresponding to that determined by Imre et al.[76] for $NH_4HSO_4 \cdot 8H_2O_{(cr)}/NH_4HSO_{4(cr)}$. This disagreement remains to be resolved by future measurements.

Calculated salt solubilities and water activities (at 298.15 K) are shown in Figure 21, which has two notable features. First, water activity/concentration relationships in the mixtures cannot be adequately approximated by interpolating between values for the pure components $(NH_4)_2SO_4-H_2O$ and $H_2SO_4-H_2O$. Even for relatively dilute solutions the variation of total solute molality (m_T) with composition is nonlinear for a fixed water activity, with a maximum occurring at a $(NH_4)_2SO_4$ fraction (r) of 0.6−0.8 (Figure 15). Second, for H_2SO_4 molalities greater than about 7.5 mol kg^{-1}, the addition of $(NH_4)_2SO_4$ causes water activity to increase rather than decrease. These effects are likely to be due to HSO_4^- formation in the solution and emphasize the importance of treating this reaction explicitly in order to predict accurately the properties of acid sulfate solutions. We note that qualitatively similar behavior is observed for $Na_2SO_4-H_2SO_4-H_2O$ mixtures.

The water activities shown in Figure 21 are similar, for most compositions, to those obtained by Clegg and Brimblecombe;[23] see their Figures 7 and 9. However, in the present model values of water activities for supersaturated aqueous $(NH_4)_2SO_4$ are

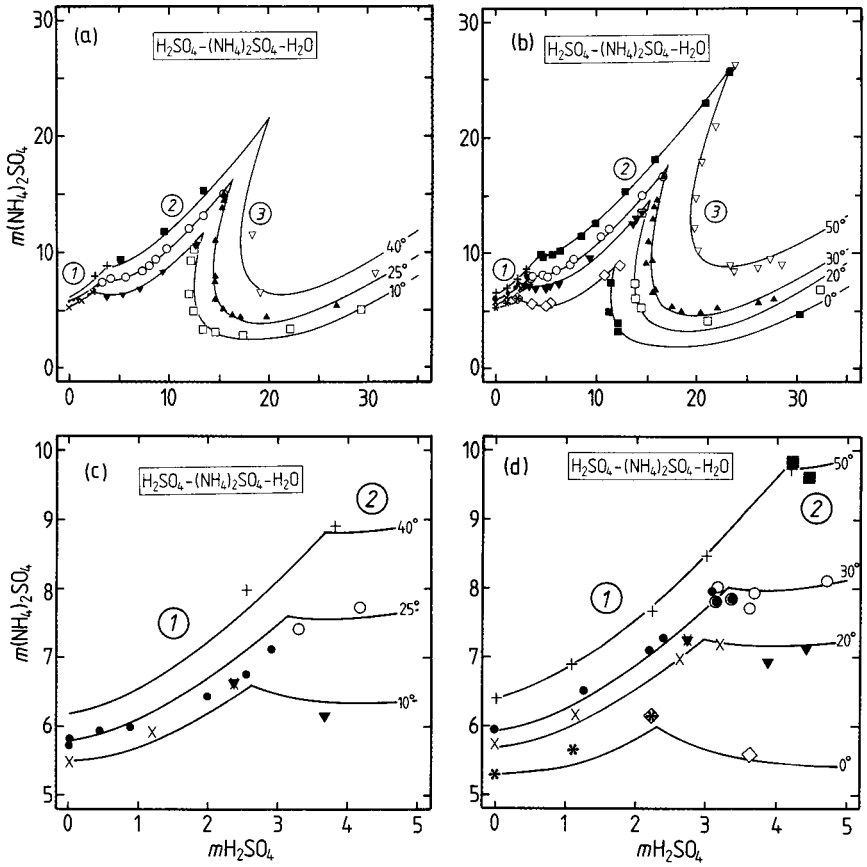

Figure 20. Salt solubilities in $H_2SO_4-(NH_4)_2SO_4-H_2O$ solutions, from 273.15 to 323.15 K, plotted as molalities. Data from Silcock.[53] (a, c) Solid phases: (1) $(NH_4)_2SO_{4(cr)}$ (crosses [283.15 K], dots [298.15 K], plusses [313.15 K]); (2) $(NH_4)_3H(SO_4)_{2(cr)}$ (inverted solid triangles [283.15 K], open circles [298.15 K], solid squares [313.15 K]); (3) $NH_4HSO_{4(cr)}$ (open squares [283.15 K], solid triangles [298.15 K], inverted open triangles [313.15 K]). (b, d) Solid phases: (1) $(NH_4)_2SO_{4(cr)}$ (asterisks [273.15 K], crosses [293.15 K], dots [303.15 K], pluses [323.15 K]); (2) $(NH_4)_3H(SO_4)_{2(cr)}$ (open diamonds [273.15 K], inverted solid triangles [293.15 K], open circles [303.15 K], solid squares [323.15 K]); (3) $NH_4HSO_{4(cr)}$ (solid squares [273.15 K], open squares [293.15 K], solid triangles [303.15 K], inverted open triangles [323.15 K]). Lines on all plots: fitted model, at the indicated Celsius temperatures.

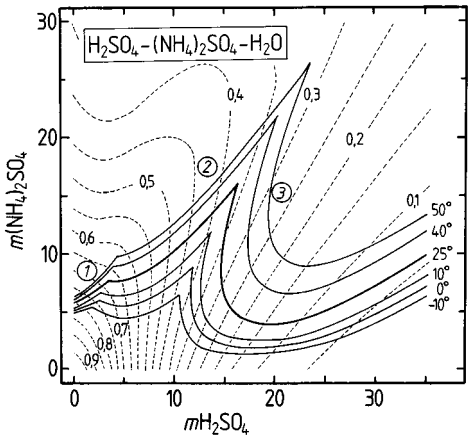

Figure 21. Phase diagram of $H_2SO_4-(NH_4)_2SO_4-H_2O$ from 263.15 to 323.15 K and equilibrium water activities for both subsaturated and supersaturated solutions at 298.15 K. Compositions are given as molalities. Lines: solid, solubilities of (1) $(NH_4)_2SO_{4(cr)}$, (2) $(NH_4)_3H(SO_4)_{2(cr)}$, and (3) $NH_4HSO_{4(cr)}$, at indicated Celsius temperatures. Contours: equilibrium water activities at 298.15 K, with values as marked.

lower, for a given molality, and this is reflected in the predicted water activities for supersaturated mixtures containing greater than about 3:1 NH_4^+/H^+. We also note that the fall and then rise of the water activity contours in this composition region (e.g., for $a_1 = 0.4$) is a consequence of the model fitting the available data at NH_4^+/H^+ ratios 1:0, 2.448:1, and 3:1. This property of the mixtures therefore appears to be real and not a model artifact.

TABLE 6: Sources of Thermodynamic Data for $NH_4NO_3-(NH_4)_2SO_4-H_2O$ Solutions[a]

m^b					
min	max	used[c]	data type[d]	t (°C)	source
5.347	65.74	yes	sol	0−70	Silcock[53]
5.805	51.4	no[e]	sol	25−105	Emons and Kloth[54]
7.68	7.68	no[e]	sol	−21	Mazzotto[52]
4.870	69.91	yes	edb[f]	25	Chan et al.[27]
5.82	25.3	no[e]	vp	25−70	Emons and Hahn[32]

[a] Parameters determined: $W_{SO4\cdot NO3\cdot NH4}$, $Q_{1,SO4\cdot NO3\cdot NH4}$, and $U_{SO4\cdot NO3\cdot NH4}$. [b] Total molality ($mNH_4NO_3 + m(NH_4)_2SO_4$). [c] Used in the fit of the model. [d] Type of measurement: sol, solubility of $NH_4NO_{3(cr)}$, $(NH_4)_2SO_{4(cr)}$, $(NH_4)_2SO_4\cdot 2NH_4NO_{3(cr)}$, $(NH_4)_2SO_4\cdot 3NH_4NO_{3(cr)}$, or ice; edb, electrodynamic balance data; vp, equilibrium partial pressures of water. [e] Only compared with the fitted model (see text). [f] These data were restandardized using water activities for subsaturated aqueous generated using the model.

3.8. $(NH_4)_2SO_4-NH_4NO_3-H_2O$. Table 6 lists the data sets available for this system, which include solubilities with respect to five solid phases, edb measurements for six different NO_3^-/SO_4^{2-} ratios, and equilibrium water vapor pressures. Below the upper temperature limit of the model (323.15 K) salt solubilities have been measured from 273.15 to 313.15 K, with a single determination by Mazzotto[52] of simultaneous saturation with respect to $NH_4NO_{3(cr)}$, $(NH_4)_2SO_{4(cr)}$, and ice at 252.15 K.

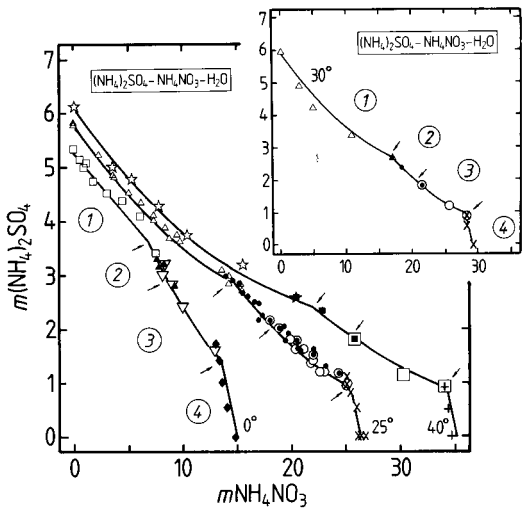

Figure 22. Salt solubilities in $(NH_4)_2SO_4-NH_4NO_3-H_2O$, from 273.15 to 313.15 K, plotted as molalities. Data from Silcock[53] and Emons and Kloth.[54] Solid phases: (1) $(NH_4)_2SO_{4(cr)}$ (stars, open triangles, open squares); (2) $(NH_4)_2SO_4 \cdot 2NH_4NO_{3(cr)}$ (solid squares, dots, solid triangles); (3) $(NH_4)_2SO_4 \cdot 3NH_4NO_{3(cr)}$ (open squares, open circles, inverted open triangles); (4) $NH_4NO_{3(cr)}$ (pluses, crosses, solid diamonds). Lines: fitted model. Arrows point to the boundaries between the different solid phases, whose order of occurrence is the same at each temperature.

The model was first fitted to the solubility data compiled by Silcock[53] with equilibrium constants of the double salts $(NH_4)_2SO_4 \cdot 2NH_4NO_{3(cr)}$ and $(NH_4)_2SO_4 \cdot 3NH_4NO_{3(cr)}$ as unknowns and to the edb measurements of Chan et al.[27] The more recent solubility determinations of Emons and Kloth[54] agree well with earlier data (from two different sources), although these authors apparently obtained $NH_4NO_{3(cr)}$ as a solid phase in a region of composition in which only the double salts should occur. Water activities derived from the vapor pressures of Emons and Hahn[32] between 298.15 and 323.15 K (using their $p°(H_2O)$) agreed with the fitted model to within +0.016 to −0.012 in a_1, a satisfactory result. A comparison with the measurement of the eutectic solution determined by Mazzotto[52] gave a predicted water activity at the freezing temperature (0.8172) within 0.0024 of the true value for −21.0 °C (calculated using the equation in Table 4 of Carslaw et al.[9]). Calculated degrees of saturation with respect to $NH_4NO_{3(cr)}$ and $(NH_4)_2SO_{4(cr)}$ were 0.70 and 1.14, respectively. The deviation is relatively large in the case of ammonium nitrate and could not be significantly improved by changes to the model parameterization. The reason for the disagreement is unclear, although calculations suggest that solutions should become saturated with respect to the two double salts at a lower NH_4NO_3 molality than for $NH_4NO_{3(cr)}$. This may not have been recognized by Mazzotto.[52]

The model fit based upon the solubilities compiled by Silcock[53]and edb data of Chan et al.[27] was accepted as the final result and is shown in Figures 22 and 23. A notable feature of the measured solubilities is that the compositions for which the two double salts occur show considerable overlap (e.g., see the plot for 298.15 K in Figure 22). Calculations suggest that this is because saturation with respect to both solid phases is closely approached over a quite wide range of composition, which would tend to facilitate precipitation of the metastable solid phase.

Fitted parameters and equilibrium constants are listed in Tables 1 and 2. Water activities and salt solubilities in the system are illustrated in Figure 24.

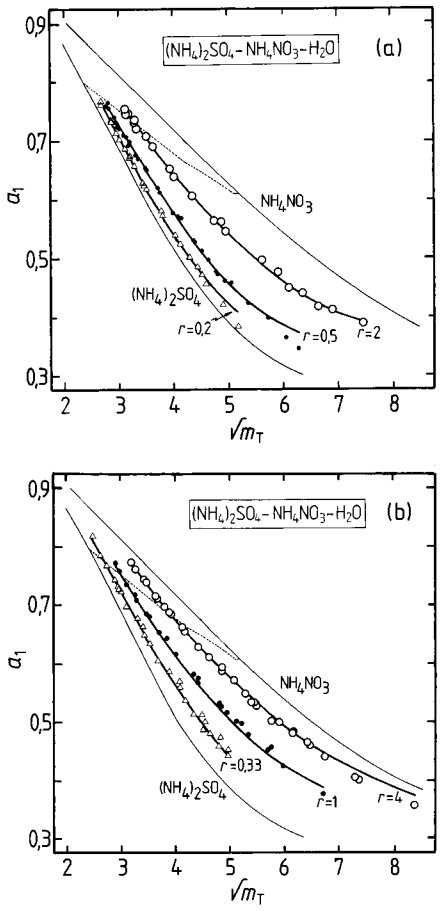

Figure 23. Water activities (a_1) of supersaturated $(NH_4)_2SO_4-NH_4NO_3-H_2O$ at 298.15 K, plotted against the square root of total molality (m_T, equivalent to $m(NH_4)_2SO_4 + mNH_4NO_3$). Data are from Chan et al.[27] Symbols: data for different ratios r (equal to $mNH_4NO_3/m(NH_4)_2SO_4$), as marked. Lines: solid (heavy), the fitted model; solid (fine), calculated a_1 for pure aqueous NH_4NO_3 and $(NH_4)_2SO_4$; dotted, calculated solubility curve (solutions are supersaturated below this line).

3.9. $NH_4HSO_4-NH_4NO_3-H_2O$. The sources of available data for this system are listed in Table 7. Highly acidic aerosols containing nitrate are unlikely to occur in the atmosphere, due to the volatility of HNO_3 at all temperatures except those encountered in the polar stratosphere. However, solubilities of $NH_4HSO_{4(cr)}$ and $NH_4HSO_4 \cdot NH_4NO_{3(cr)}$ are useful in constraining the model with respect to $NH_4^+-HSO_4^--NO_3^-$ interactions, and the equilibrium constant of the acid double salt was therefore determined.

The model was fitted to the 14 available measurements from 283.15 to 323.15 K, and the results are shown in Figure 25. The solubilities of three solid phases have been measured at 298.15 K ($NH_4HSO_{4(cr)}$, $NH_4NO_{3(cr)}$, and $NH_4HSO_4 \cdot NH_4NO_{3(cr)}$). The increase of $NH_4NO_{3(cr)}$ solubility with NH_4HSO_4 molality (Figure 25a) is accurately represented by the model, and the measured values are consistent with that for pure aqueous NH_4NO_3 (26.8 mol kg^{-1}). However, this is not the case for $NH_4HSO_{4(cr)}$: the measured solubilities are lower than predicted, even for pure aqueous NH_4HSO_4 (see also Figure 21). It is also apparent that letovicite should precipitate at a lower NH_4HSO_4 molality (solid line 1 in Figure 25a) than either $NH_4HSO_{4(cr)}$ or $NH_4HSO_4 \cdot NH_4NO_{3(cr)}$. Both of these solid phases therefore appear to be metastable in this system. The change in solubility of $NH_4HSO_4 \cdot NH_4NO_{3(cr)}$ with temperature, Figure 25b, is adequately represented by the model over a 30

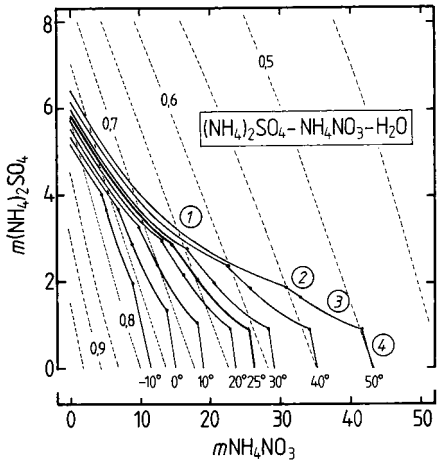

Figure 24. Phase diagram of $(NH_4)_2SO_4-NH_4NO_3-H_2O$ from 263.15 to 323.15 K, and equilibrium water activities for both subsaturated and supersaturated solutions at 298.15 K. Compositions are given as molalities. Lines: solid, solubilities of the following solid phases at the indicated Celsius temperatures: (1) $(NH_4)_2SO_{4(cr)}$, (2) $(NH_4)_2SO_4 \cdot 2NH_4NO_{3(cr)}$, (3) $(NH_4)_2SO_4 \cdot 3NH_4NO_{3(cr)}$, (4) $NH_4NO_{3(cr)}$. Dots on the lines indicate the boundaries between the solid phases. Dashed contours: equilibrium water activities (a_1) at 298.15 K, with values as marked.

TABLE 7: Sources of Thermodynamic Data for $NH_4NO_3-NH_4HSO_4-H_2O$ Solutions[a]

m[b] min	m[b] max	composition	used[c]	data[d] type	t (°C)	source
32.079	64.783	*e*	yes	sol	25	Silcock[53]
49.684	>100	*e*	yes	sol	20−60	Linke[26]

[a] Parameter determined: $W_{HSO4\cdot NO3\cdot NH4}$. [b] Total molality ($m NH_4NO_3 + m(NH_4)_2SO_4 + m H_2SO_4$). [c] Used in the fit of the model. [d] Type of measurement: sol, solubility of $NH_4NO_{3(cr)}$, $NH_4HSO_{4(cr)}$, or $NH_4HSO_4 \cdot NH_4NO_{3(cr)}$. [e] Mixtures of aqueous NH_4NO_3 and NH_4HSO_4, in various proportions.

K range of temperature, though the uncertainty of ${}^xK_S(NH_4HSO_4 \cdot NH_4NO_3)$ at 298.15 K is at least ±10% and probably greater (see the dotted lines in Figure 25a).

Water activities and salt solubilities in the system are illustrated in Figure 26, and fitted model parameters and equilibrium constant of $NH_4HSO_4 \cdot NH_4NO_{3(cr)}$ are given in Tables 1 and 2.

4. Discussion

The model parameterization for the atmospherically important $H_2SO_4-(NH_4)_2SO_4-H_2O$ system is based chiefly upon vapor pressures (including edb measurements) at 298.15 K, salt solubilities from 273.15 to 323.15 K, and isopiestic data for relatively dilute solutions ($a_1 \geq 0.775$) at 298.15 and 323.15 K. The available measurements are sufficient to define adequately the thermodynamic properties at 298.15 K over most of the composition range. This is even true of supersaturated solutions, though with the reservation that there remain some inconsistencies between the edb data obtained by different groups (see Figure 14). However, the variation of ion and solvent activities with temperature is poorly defined, and the parameterization presented here is unlikely to be unique even though the model quite accurately represents the available solubilities and isopiestic data at 323.15 K. Measurements of the thermal properties (enthalpies of dilution and heat capacities) of the system would be valuable, over a range of compositions, and also determinations of phase equilibria at low temperatures. Calculated phase diagrams of $H_2SO_4-(NH_4)_2SO_4-H_2O$ mixtures from 253.15 to 223.15 K are shown in Figure 27, with contours of equilibrium relative humidity (water activity) superimposed. It is clear that the presence of $(NH_4)_2SO_4$ in the aqueous phase at concentrations on the order of a few mol kg^{-1} has relatively little influence on the water activity of an

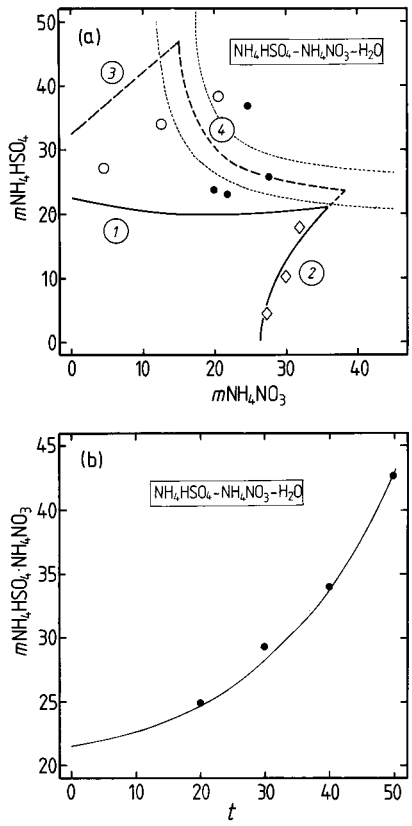

Figure 25. (a) Salt solubilities in $NH_4HSO_4-NH_4NO_3-H_2O$ at 298.15 K, plotted as molalities. Data from Silcock.[53] Solid phases: (1) $(NH_4)_3H(SO_4)_{2(cr)}$ (calculated); (2) $NH_4NO_{3(cr)}$ (open diamonds); (3) $NH_4HSO_{4(cr)}$ (open circles); (4) $NH_4HSO_4 \cdot NH_4NO_{3(cr)}$ (dots). Lines: solid, saturation with respect to solids $(NH_4)_3H(SO_4)_{2(cr)}$ and $NH_4NO_{3(cr)}$; dashed, saturation with respect to $NH_4HSO_{4(cr)}$ and $NH_4HSO_4 \cdot NH_4NO_{3(cr)}$; dotted, saturation with respect $NH_4HSO_4 \cdot NH_4NO_{3(cr)}$ for changes of ±10% in the equilibrium constant. (b) The solubility of $NH_4HSO_4 \cdot NH_4NO_{3(cr)}$ (mol kg^{-1}) as a function of temperature (t/°C). Symbols: data from Linke.[26] Line: fitted model.

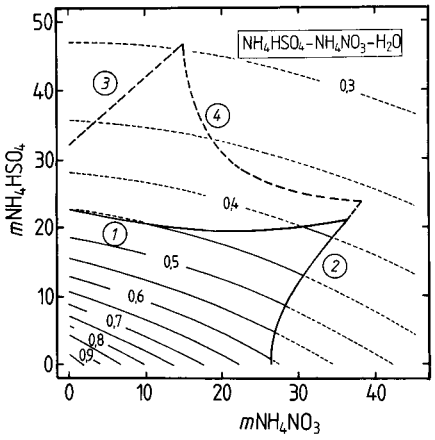

Figure 26. Phase diagram of $NH_4HSO_4-NH_4NO_3-H_2O$ at 298.15 K and equilibrium water activities for both subsaturated and supersaturated solutions. Compositions are given as molalities. Lines: solid (heavy), solubilities of (1) $(NH_4)_3H(SO_4)_{2(cr)}$, (2) $NH_4NO_{3(cr)}$; dashed (heavy), (3) $NH_4HSO_{4(cr)}$, (4) $NH_4HSO_4 \cdot NH_4NO_{3(cr)}$. Contours: equilibrium water activities, with values as marked. Contours are dotted for supersaturated solutions.

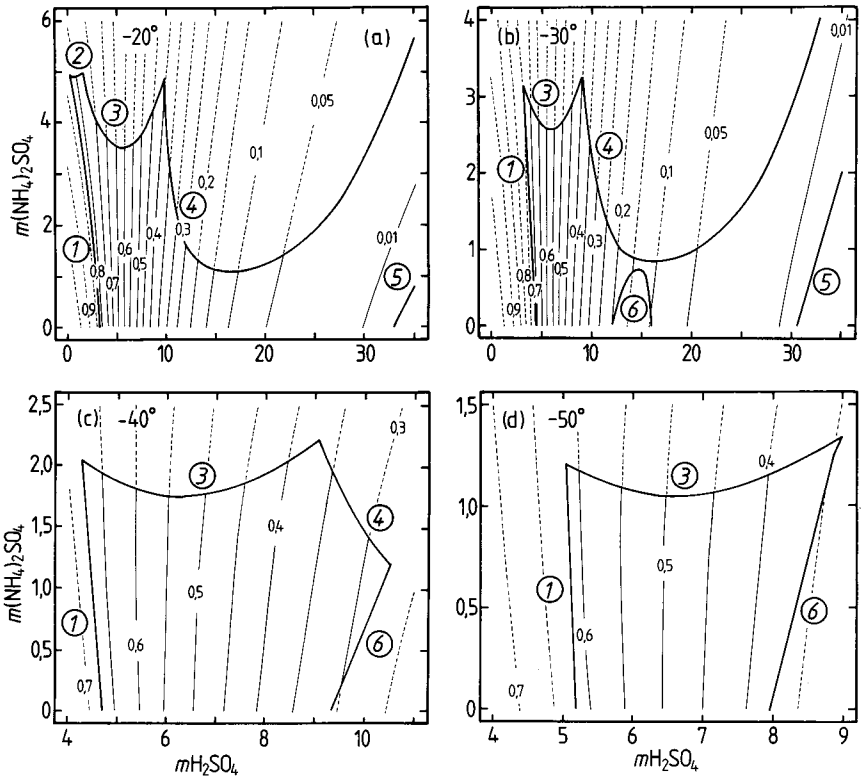

Figure 27. Phase diagram of $H_2SO_4-(NH_4)_2SO_4-H_2O$ from 223.15 to 253.15 K and equilibrium water activities for both subsaturated and supersaturated solutions. Compositions are given as molalities. Lines: solid (heavy), saturation with respect to (1) ice, (2) $(NH_4)_2SO_{4(cr)}$, (3) $(NH_4)_3H(SO_4)_{2(cr)}$, (4) $NH_4HSO_{4(cr)}$, (5) $H_2SO_4 \cdot H_2O_{(cr)}$, (6) $H_2SO_4 \cdot 4H_2O_{(cr)}$. Contours: equilibrium water activities (dashed for supersaturated solutions), with values as marked. (a) 253.15 K; (b) 243.15 K; (c) 233.15 K; (d) 223.15 K.

$H_2SO_4-H_2O$ solution, although in highly concentrated solutions it is increased by the addition of $(NH_4)_2SO_4$. This implies that in the atmosphere an aqueous aerosol containing both $(NH_4)_2SO_4$ and H_2SO_4 could be more highly concentrated with respect to H_2SO_4 than a pure aqueous H_2SO_4 aerosol. This could affect the rates of some reactions that occur in, or on the surface of, aqueous acidic aerosols. Figure 27c,d shows that, at 233.15 and 223.15 K, the range of humidity and $(NH_4)_2SO_4$ molality of the stable liquid region is small. It is thought that aerosols in the stratosphere can become supersaturated with respect to H_2SO_4 and HNO_3 hydrates[8] and remain liquid. Aerosols of $H_2SO_4-(NH_4)_2SO_4-H_2O$ composition are readily maintained in the laboratory in a supersaturated state, and it seems reasonable to suppose that such liquid aerosols may also occur in the atmosphere. The properties of supersaturated solutions predicted by the model are subject to a large uncertainty at temperatures far from 298.15 K since the edb data that constrain the fits are currently restricted to this temperature.

Equilibrium partial pressures of NH_3 over aqueous solutions containing $NH_4^+{}_{(aq)}$ can be calculated using eq 11b and for $H_2SO_4-(NH_4)_2SO_4-H_2O$ mixtures are very low: about 10^{-11} atm for a 6 mol kg^{-1} solution of aqueous NH_4HSO_4 (see Figure 10 of Clegg and Brimblecombe[23]). How accurate are values of $p$$NH_3$ predicted by the model? Clegg and Brimblecombe[23] have compared their results with the data of Koutrakis and Aurian-Blajeni,[55] although there appear to be errors in the calibration of their experiments (see section 4 of Clegg and Brimblecombe[23]). Agreement is poor. Given that the equilibrium constant for the reaction in eq 11 is well-determined (from values of the Henry's law constant and the acid dissociation constant of $NH_4^+{}_{(aq)}$), the overall accuracy of predicted $p$$NH_3$ is limited chiefly by the ability of the model to predict the quantity $a$$NH_4^+/a$$H^+$. At present, as the dissociation of water into $H^+{}_{(aq)}$ and $OH^-{}_{(aq)}$ is not treated by the model, these predictions are restricted to acid solutions (about pH 5 and below, where the dissociation of water is suppressed). Maeda and Iwata[56] have measured the pK_a* of $NH_4^+{}_{(aq)}$ in aqueous $(NH_4)_2SO_4$ at 298.15 K. The model of Clegg et al.[25] is able to reproduce the data to within experimental precision when combined with critically assessed estimates of the activity coefficient of NH_3 in aqueous $(NH_4)_2SO_4$.[17] We have compared values of $a$$NH_4^+/a$$H^+$ predicted by the equations of Clegg et al.[25] and the present model, for aqueous $(NH_4)_2SO_4$ solutions containing 10^{-4} mol kg^{-1} H_2SO_4. There is agreement to within 2% at 6 mol kg^{-1} $(NH_4)_2SO_4$ (79% relative humidity), decreasing to about 30% for 0.5 mol kg^{-1} $(NH_4)_2SO_4$ (98% relative humidity). While this comparison is limited, the result gives reasonable confidence in predictions of $p$$NH_3$.

It has been suggested that ternary homogeneous nucleation of $H_2SO_4-(NH_4)_2SO_4-H_2O$ aerosols may occur in the atmosphere,[2] and methods for estimating the rate of this process require a knowledge of the equilibrium partial pressure of H_2SO_4 above the solutions. Recently, Marti et al.[57] have determined $p$$H_2SO_4$ over $H_2SO_4-(NH_4)_2SO_4-H_2O$ solutions at 303.15 K by measuring the rate of evaporation of H_2SO_4 from aerosol droplets for different liquid-phase ion ratios NH_4^+/SO_4^{2-} and for relative humidities from 2.9 to 14.4%. For solutions rich in NH_4^+ the concentrations reached in aqueous solutions at some of these relative humidities are beyond the limit of the model. However, it is worthwhile to compare predicted $p$$H_2SO_4$ with the data of Marti et al.[57] First, a Henry's law constant of 5×10^{11} atm^{-1} at 303.15 K (for the reaction $H_2SO_{4(g)} \rightleftharpoons 2H^+{}_{(aq)} + SO_4^{2-}{}_{(aq)}$) was estimated from the vapor pressure equation of Ayers et al.[58] and aqueous activities tabulated by Giauque et al.[59] For each of the NH_4^+/SO_4^{2-} ratios listed in Table 4 of Marti et al.[57] the model was used to calculate first the aqueous

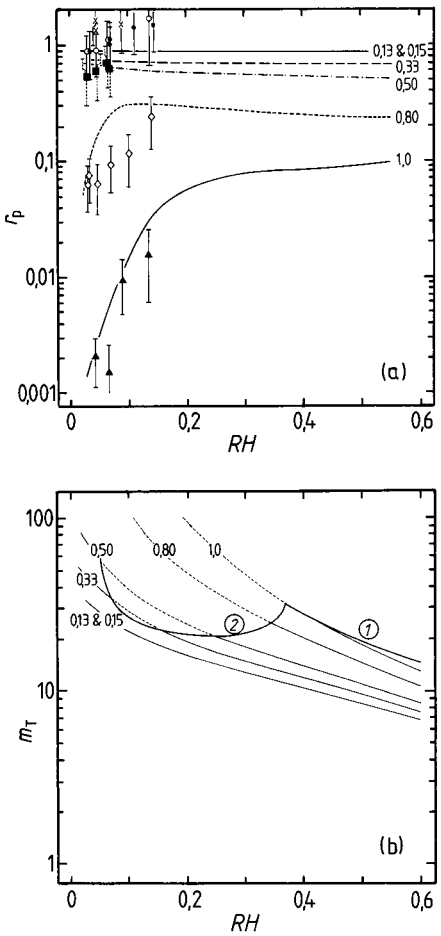

Figure 28. Partial pressures of H_2SO_4 over $H_2SO_4-(NH_4)_2SO_4-H_2O$ mixtures at 303.15 K. (a) The ratio (r_p) of pH_2SO_4 over the aqueous mixture to that over pure aqueous H_2SO_4 at the same relative humidity (*RH*), plotted as a function of *RH*. Data are from Marti et al.[57] Symbols are experimental results for the following molar NH_4^+/SO_4^{2-} ratios: crosses, 0.13; dots, 0.15; open circles, 0.33; solid squares, 0.50; open diamonds, 0.80; solid triangles, 1.0. Lines: calculated using the model for each NH_4^+/SO_4^{2-} ratio (indicated on the plot). (b) Calculated total molalities (m_T, equal to $mH_2SO_4 + m(NH_4)_2SO_4$) for each NH_4^+/SO_4^{2-} ratio, as a function of relative humidity. The saturation curve is also shown, for solid phases $(NH_4)_3H(SO_4)_{2(cr)}$ (1) and $NH_4HSO_{4(cr)}$ (2). Values of m_T for supersaturated solutions are plotted as dotted lines.

phase concentration for the listed relative humidity and then pH_2SO_4 from the H^+ and SO_4^{2-} activities. The measured partial pressures cover a 4 order of magnitude range. These are compared with model predictions in Figure 28 as the ratio of the equilibrium partial pressure over the mixed solution to that over pure aqueous H_2SO_4 at the same relative humidity and temperature. The data and predicted pressure ratios are consistent and show, first, that for low ratios of NH_4^+/SO_4^{2-} the partial pressure of H_2SO_4 is hardly reduced from that over the pure aqueous acid: for NH_4^+/SO_4^{2-} up to about 0.5 the decrease is no more than a factor of 2. Second, the trend in pH_2SO_4 (and r_p, the quantity plotted in Figure 28a) for NH_4^+/SO_4^{2-} ratios of 0.8 and 1.0 is correctly predicted by the model. Quantitative agreement is good even though the model is being extrapolated beyond the limits of its validity. Calculated total solute molalities for each ion ratio are shown in Figure 28b, with the saturation curve superimposed. Some of the aerosols measured by Marti et al. (1997) appear to be supersaturated with respect to $NH_4HSO_{4(cr)}$, and concentrations in the 0.8 and 1.0 NH_4^+/SO_4^{2-} solutions exceed 100 mol kg^{-1} at the relative humidities for which pH_2SO_4 was measured. Given the difficulties of measuring partial pressures of H_2SO_4 (only 1.4×10^{-6} to 6.8×10^{-11} Pa in the experiments of Marti et al.[57]) and the very high concentrations in the aerosol solutions, the overall agreement is satisfactory.

TABLE 8: Gibbs Energies and Enthalpies of Formation of Acid Ammonium Sulfate Salts and Nitrate−Sulfate Double Salts[a]

salt	$\Delta_fG°$ (kJ mol^{-1})	$\Delta_fH°$ (kJ mol^{-1})
$(NH_4)_3H(SO_4)_2$	−1791.46	−2210
NH_4HSO_4	−852.12	−1027
$(NH_4)_2SO_4 \cdot 2NH_4NO_3$	−1342.97 (−1341.3)	−1913 (−1912)
$(NH_4)_2SO_4 \cdot 3NH_4NO_3$	−1547.77 (−1545.6)	−2279 (−2277)
$NH_4HSO_4 \cdot NH_4NO_3$	−1009.44 (−1056.4)	−1390 (−1392)

[a] The first value listed for each salt was calculated from the equilibrium constant given in Table 2, together with $\Delta_fG°$ or $\Delta_fH°$ for the ions from Wagman et al.[19] and standard thermodynamic relations. The values in parentheses are estimates obtained by adding $\Delta_fG°$ and $\Delta_fH°$ for the individual salts $(NH_4)_2SO_{4(cr)}$, $NH_4NO_{3(cr)}$, and $NH_4HSO_{4(cr)}$ in the appropriate multiples (e.g., $\Delta_fG°(NH_4HSO_4 \cdot NH_4NO_{3(cr)}) = \Delta_fG°(NH_4NO_{3(cr)}) + \Delta_fG°(NH_4HSO_{4(cr)})$).

In the atmosphere, exchanges of $NH_{3(g)}$ and $HNO_{3(g)}$ between the gas phase and solid NH_4NO_3 particles may lead to the following equilibrium being established:

$$NH_4NO_{3(cr)} \rightleftharpoons NH_{3(g)} + HNO_{3(g)} \quad (17a)$$

$$K_p(NH_4NO_3) = pNH_3 pHNO_3 \quad (17b)$$

where K_p (atm^2) is the equilibrium constant, which can be expressed as

$$K_p(NH_4NO_3) = {}^xK_S(NH_4NO_3)/({}^x\boldsymbol{K}'_H(NH_3)\,{}^xK_H(HNO_3)) \quad (18)$$

Combining values from eqs 12 and 15 and Table 3, we obtain $K_p(NH_4NO_3)$ at 298.15 K equal to 4.36×10^{-17} atm^2 (4.48×10^{-17} bar^2) and an enthalpy change ($\Delta_rH°$) equal to 184.2 kJ mol^{-1}. These agree closely with the evaluation of Mozurkewich,[60] who obtained $K_p(NH_4NO_3)$ equal to $(43 \pm 5) \times 10^{-18}$ bar^2 and an enthalpy change of 185.3 kJ mol^{-1} at 298.15 K for the reaction in eq 17.

Finally, we note that application of the model to the $(NH_4)_2SO_4-NH_4NO_3-H_2O$ and $NH_4HSO_4-NH_4NO_3-H_2O$ systems has enabled equilibrium constants for the formation of the double salts $(NH_4)_2SO_4 \cdot 2NH_4NO_{3(cr)}$, $(NH_4)_2SO_4 \cdot 3NH_4NO_{3(cr)}$, and $NH_4HSO_4 \cdot NH_4NO_{3(cr)}$ to be determined. Values of $\Delta_fG°$ and $\Delta_fH°$ for the solid phases are given in Table 8 and are compared with estimates obtained from a linear combination of $\Delta_fG°$ and $\Delta_fH°$ for the salts $(NH_4)_2SO_{4(cr)}$, $NH_4NO_{3(cr)}$, and $NH_4HSO_{4(cr)}$. Details of the calculation are given in the notes to Table 8. For the two nitrate/sulfate double salts agreement is surprisingly good, with differences of less than 2.2 kJ mol^{-1} for both $\Delta_fG°$ and $\Delta_fH°$. The discrepancy is greatest for $NH_4HSO_4 \cdot NH_4NO_{3(cr)}$, whose equilibrium constant is subject to a larger uncertainty (section 3.9). The thermodynamic properties of $(NH_4)_3H(SO_4)_{2(cr)}$ and $NH_4HSO_{4(cr)}$ are also given in Table 8. The value of $\Delta_fH°$ for $NH_4HSO_{4(cr)}$ differs by only 0.36 kJ mol^{-1} from the value tabulated by Wagman et al.[19]

5. Summary

The mole-fraction-based thermodynamic model presented here provides a self-consistent representation of ion and solvent activities in $H^+-NH_4^+-NO_3^--SO_4^{2-}-H_2O$ mixtures to high supersaturation, for temperatures up to 328.15 K. The model has been parameterized using available vapor pressures, isopiestic and edb data, degrees of dissociation, emfs, and pK_a*

measurements. For the pure aqueous acids and their mixtures the model is identical to that of Carslaw et al.[9]

The model reproduces the measured thermodynamic properties of $H_2SO_4-(NH_4)_2SO_4-H_2O$ mixtures well, although the available data are confined to temperatures of 273.15 K and above. Further determinations of activities, thermal properties, and solid/liquid phase equilibria for $H_2SO_4-(NH_4)_2SO_4-H_2O$ mixtures would be worthwhile to constrain better the model for this important atmospheric system at low temperatures.

Gibbs energies and enthalpies of formation for acid ammonium sulfate and sulfate−nitrate double salts have been calculated from the equilibrium constants for dissolution of the solid phases, and the results are consistent with estimates obtained from values for the individual component salts.

Measurements of equilibrium partial pressures of NH_3 and H_2SO_4 over acidic solutions are sparse. However, comparisons with existing data for the activities required to calculate pNH_3 and with determinations of pH_2SO_4 suggest that the model can be used (with the necessary equilibrium constants) to calculate these quantities with satisfactory accuracy.

Note: FORTRAN code implementing the model described here is available from S. Clegg (s.clegg@uea.ac.uk) and can also be run from the following websites: http://www.uea.ac.uk/~e770/aim.html, and http://www.me.udel.edu/wexler/aim.html.

Acknowledgment. This work was funded by a NATO Collaborative Research Grant (CRG 960160). We also wish to acknowledge the support of the Natural Environment Research Council (Advanced Fellowship GT5/93/AAPS/2 for S.L.C.) and a grant from the IBM Environmental Research Programme.

References and Notes

(1) Easter, R. C.; Peters, L. K. *J. Appl. Met.* **1994**, *33*, 775−784.
(2) Coffman, D. J.; Hegg, D. A. *J. Geophys. Res.* **1995**, *100*, 7147−7160.
(3) Seinfeld, J. H. *Atmospheric Chemistry and Physics of Air Pollution*; John Wiley and Sons: New York, 1986.
(4) Pilinis, C.; Seinfeld, J. H.; Seigneur, C. *Atmos. Environ.* **1987**, *21*, 943−955.
(5) Pilinis, C.; Pandis, S. N.; Seinfeld, J. H. *J. Geophys. Res.* **1995**, *100*, 18739−18754.
(6) Tang, I. N.; Munkelwitz, H. R. *J. Geophys. Res.* **1994**, *99*, 18801−18808.
(7) Rood, M. J.; Shaw, M. A.; Larson, T. V. *Nature* **1989**, *337*, 537−539.
(8) Carslaw, K. S.; Luo, B. P.; Clegg, S. L.; Peter, Th.; Brimblecombe, P.; Crutzen, P. J. *Geophys. Res. Lett.* **1994**, *21*, 2479−2482.
(9) Carslaw, K. S.; Clegg, S. L.; Brimblecombe, P. *J. Phys. Chem.* **1995**, *99*, 11557−11574.
(10) Clegg, S. L.; Pitzer, K. S.; Brimblecombe, P. *J. Phys. Chem.* **1992**, *96*, 9470−9479; **1994**, *98*, 1368; **1995**, *99*, 6755.
(11) Carslaw, K. S.; Peter, T.; Clegg, S. L. *Rev. Geophys.* **1997**, *35*, 125−154.
(12) Robinson, R. A.; Stokes, R. H. *Electrolyte Solutions*, 2nd ed. (revised); Butterworths: London, 1965.
(13) Young, T. F.; Maranville, L. F.; Smith, H. M. In *Structure of Electrolytic Solutions*; Hamer, W. J., Ed.; Wiley: New York, 1959; pp 35−63.
(14) Clegg, S. L.; Brimblecombe, P. *J. Chem. Eng. Data* **1995**, *40*, 43−64.
(15) Clegg, S. L.; Brimblecombe, P. *J. Phys. Chem.* **1990**, *94*, 5369−5380; **1992**, *96*, 6854.
(16) Clegg, S. L.; Whitfield, M. *Geochim. et Cosmochim. Acta* **1995**, *59*, 2403−2421.
(17) Clegg, S. L.; Brimblecombe, P. *J. Phys. Chem.* **1989**, *93*, 7237−7248.
(18) Stull, D. R.; Prophet, H. *JANAF Thermochemical Tables*, Report NSRDS-NBS-37; US Govt. Printing Office: Washington, DC, 1971.
(19) Wagman, D. D.; Evans, W. H.; Parker, V. B.; Schumm, I. H.; Bailey, S. M.; Churney, K. L.; Nuttall, R. L. *J. Phys. Chem. Ref. Data* **1982**, *11*, 1−392.
(20) Roux, A.; Musbally, G. M.; Perron, G.; Desnoyers, J. E.; Singh, P. P.; Woolley, E. M.; Hepler, L. G. *Can. J. Chem.* **1978**, *56*, 24−28.
(21) Pitzer, K. S. In *Activity Coefficients in Electrolyte Solutions*, 2nd ed.; Pitzer, K. S., Ed.; CRC Press: Boca Raton, 1991; pp 75−153.
(22) Clegg, S. L.; Ho, S. S.; Chan, C. K.; Brimblecombe, P. *J. Chem. Eng. Data* **1995**, *40*, 1079−1090.
(23) Clegg, S. L.; Brimblecombe, P. *J. Aerosol Sci.* **1995**, *26*, 19−38.
(24) Clegg, S. L.; Brimblecombe, P.; Liang, Z.; Chan, C. K. *Aerosol Sci. Technol.* **1997**, *27*, 345−366.
(25) Clegg, S. L.; Milioto, S.; Palmer, D. A. *J. Chem. Eng. Data* **1996**, *41*, 455−467.
(26) Linke, W. F. *Solubilities of Inorganic and Metal Organic Compounds*; American Chemical Society: Washington, DC, 1965; Vol. I.
(27) Chan, C. K.; Flagan, R. C.; Seinfeld, J. H. *Atmos. Environ.* **1992**, *26A*, 1661−1673.
(28) Campbell, A. N.; Fishman, J. B.; Rutherford, G.; Schaefer, T. P.; Ross L. *Can. J. Chem.* **1956**, *34*, 151−159.
(29) Othmer, D. F.; Frohlich, G. J. *AIChE J.* **1960**, *6*, 210−214.
(30) Sacchetto, G. A.; Bombi, G. G.; Macca, C. *J. Chem. Thermodyn.* **1981**, *13*, 31−40.
(31) Parker, V. B. *Thermal Properties of Aqueous Uni-univalent Electrolytes*, Report NSRDS-NBS 2, U.S. Govt. Printing Office: Washington, DC, 1965.
(32) Emons, H. H.; Hahn, W. *Wissenschaftl. Zeitschr.* **1970**, *12*, 129−132.
(33) Vanderzee, C. E.; Waugh, D. H.; Haas, N. C. *J. Chem. Thermodyn.* **1980**, *12*, 21−25.
(34) Epikhin, Yu. A.; Bazlova, I. V.; Karapet'yants, M. Kh. *Russ. J. Phys. Chem.* **1977**, *51*, 676−677.
(35) Gladushko, V. I.; Bochenko, G. A.; Prokof'eva, G. N.; Privalko, V. P.; Vinarcik, J. *Inzh. Fiz. Zh.* **1985**, *48*, 90−91.
(36) Sorina, G. A.; Kozlovskaya, G. M.; Tsekhanskaya, Yu. V.; Bezlyudova, L. I.; Shmakov, N. G. *Zh. Fiz. Khim.* **1977**, *51*, 2099−2100.
(37) Hejtmankova, J.; Siskova, M.; Bartovska, L. *Sb. Vys. Sk. Chem. Technol. Praze, Fiz. Chem.* **1986**, 5−17.
(38) Nagatani, M.; Seiyama, T.; Sakiyama, M.; Suga, H.; Seki, S. *Bull. Chem. Soc. Jpn.* **1967**, *40*, 1833−1844.
(39) Vanderzee, C. E.; Waugh, D. H.; Haas, N. C.; Wigg, D. A. *J. Chem. Thermodyn.* **1980**, *12*, 27−40.
(40) Medvedev, V. A.; Efimov, M. E.; Cerutti, P. J.; McKay, R. M.; Johnson, L. H.; Hepler, L. G. *Thermochim. Acta* **1978**, *23*, 87−92.
(41) Treushchenko, N. N.; Pozin, M. E.; Bel'chenko, G. V.; Ivanova, E. Ya. *Zh. Prikl. Khim.* **1971**, *44*, 1753−1760.
(42) Flatt, R.; Benguerel, F. *Helvetica Chim. Acta* **1962**, *45*, 1772−1776.
(43) Kurnakov, N. S.; Ravitch, M. I. *Izv. Inst. Fiz.-Khim. Anal., Akad. Nauk SSSR* **1933**, *6*, 169−184.
(44) Maeda, M.; Kato, K. *J. Chem. Eng. Data* **1995**, *40*, 253−256.
(45) Vandoni, R. *Mem. Serv. Chim. Etat* **1944**, *31*, 87−111.
(46) Zhang, R. Y.; Wooldridge, P. J.; Molina, M. J. *J. Phys. Chem.* **1993**, *97*, 8541−8548.
(47) Richardson, R. A.; Spann, J. F. *J. Aerosol Sci.* **1984**, *15*, 563−571.
(48) Spann, J. F. Ph.D. Thesis, University of Arkansas, Fayetteville, 1984.
(49) Kim, Y. P.; Pun, B. K.-L.; Chan, C. K.; Flagan, R. C.; Seinfeld, J. H. *Aerosol Sci. Technol.* **1994**, *20*, 275−284.
(50) Park, S. K.; Awakura, Y.; Majima, H. *Metal. Trans.* **1989**, *20B*, 13−20.
(51) Tang, I. N.; Munkelwitz, H. R. *J. Aerosol Sci.* **1977**, *8*, 321−330.
(52) Mazzotto, D. *Nuovo Cimento* [3] **1891**, *29*, 21−36.
(53) Silcock, H. L. *Solubilities of Inorganic and Organic Compounds*; Pergamon: Oxford, 1979; Vol. 3.
(54) Emons, H. H.; Kloth, H. *Wissenschaftl. Zeitschr.* **1968**, *10*, 102−106.
(55) Koutrakis, P.; Aurian-Blajeni, B. *J. Geophys. Res.* **1993**, *98*, 2941−2948.
(56) Maeda, M.; Iwata, T. *J. Chem. Eng. Data* **1997**, *42*, 1216−1218.
(57) Marti, J. J.; Jefferson, A.; Cai, X. P.; Richert, C.; McMurry, P. H.; Eisele, F. *J. Geophys. Res.* **1997**, *102*, 3725−3735.
(58) Ayers, G. P.; Gillett, R. W.; Gras, J. L. *Geophys. Res. Lett.* **1980**, *7*, 433−436.
(59) Giauque, W. F.; Hornung, E. W.; Kunzler, J. E.; Rubin, T. R. *J. Am. Chem. Soc.* **1960**, *82*, 62−70.
(60) Mozurkewich, M. *Atmos. Environ.* **1993**, *27A*, 261−270.
(61) Hamer, W. J.; Wu, Y. *J. Phys. Chem. Ref. Data* **1972**, *1*, 1047−1099.
(62) Wishaw, B. F.; Stokes, R. H. *Trans. Faraday Soc.* **1952**, *48*, 27−31.
(63) Kirgintsev, A.; Lukyanov, A. V. *Russ. J. Phys. Chem.* **1965**, *39*, 653−655.
(64) Edgar, G.; Swan, W. O. *J. Am. Chem. Soc.* **1922**, *44*, 570−577.

(65) Prideaux, E. B. R.; Caven, R. M. *J. Soc. Chem. Ind.* **1919**, *39*, 353T.
(66) Prideaux, E. B. R. *J. Chem. Soc. (Ind. Trans.)* **1920**, *39*, 182T−185T.
(67) Apelblat, A. *J. Chem. Thermodyn.* **1993**, *25*, 63−71.
(68) Adams, J. R.; Merz, A. R. *Ind. Eng. Chem.* **1929**, *21*, 305−307.
(69) Janecke, E.; Rahlfs, E. *Z. Anorg. Allg. Chem.* **1930**, *192*, 237−244.
(70) Tang, I. N.; Munkelwitz, H. R.; Davis, J. G. *J. Aerosol Sci.* **1978**, *9*, 505−511.
(71) Dawson, B. S. W.; Irish, D. E.; Toogood, G. E. *J. Phys. Chem.* **1986**, *90*, 334−341.
(72) Dingemans, P. *Recl. Trav. Chim.* **1941**, *60*, 317−328.
(73) Irish, D. E.; Chen, H. *J. Phys. Chem.* **1970**, *74*, 3796−3801.
(74) Kruus, P.; Hayes, A. C.; Adams, W. A. *J. Solution Chem.* **1985**, *14*, 117−128.
(75) Balej, J.; Hanousek, F.; Pisarcik, M.; Sarka, K. *J. Chem. Soc., Faraday Trans. 1* **1984**, *80*, 521−529.
(76) Imre, D. G.; Xu, J.; Tang, I. N.; McGraw, R. *J. Phys. Chem.* **1997**, *101*, 4191−4195.